Supplementary Information for:

TRPA1 underlies a sensing mechanism for O_2

Nobuaki Takahashi[1,2], Tomoyuki Kuwaki[3], Shigeki Kiyonaka[1,4], Tomohiro Numata[1], Daisuke Kozai[1], Yusuke Mizuno[1], Shinichiro Yamamoto[1], Shinji Naito[5], Ellen Knevels[6,7], Peter Carmeliet[6,7], Toru Oga[8], Shuji Kaneko[9], Seiji Suga[10], Toshiki Nokami[10], Jun-ichi Yoshida[10] & Yasuo Mori[1,4*]

[1]Laboratory of Molecular Biology, Department of Synthetic Chemistry and Biological Chemistry, Graduate School of Engineering, and Laboratory of Environmental Systems Biology, Department of Technology and Ecology, Hall of Global Environmental Studies, Kyoto University, Kyoto 615-8510, Japan

[2]Advanced Biomedical Engineering Research Unit, Kyoto University, Kyoto 615-8510, Japan

[3]Department of Physiology, Graduate School of Medical and Dental Sciences, Kagoshima University, Kagoshima 890-8544, Japan

[4]CREST, JST, Chiyoda-ku, Tokyo 102-0075, Japan

[5]Division of Pathology, Research Laboratory, National Ureshino Hospital, Ureshino 843-0393, Japan

[6]Vesalius Research Center, Katholieke Universiteit Leuven, 3000 Leuven, Belgium

[7]Vesalius Research Center, Flanders Institute for Biotechnology (VIB), 3000 Leuven, Belgium

[8]Department of Respiratory Care and Sleep Control Medicine, Graduate School of Medicine, Kyoto University, Kyoto 606-8507, Japan

Nature Chemical Biology: doi:10.1038/nchembio.640

[9]Department of Molecular Pharmacology, Graduate School of Pharmaceutical Sciences, Kyoto University, Kyoto 606-8501, Japan

[10]Laboratory of Synthetic Organic Chemistry, Department of Synthetic Chemistry and Biological Chemistry, Graduate School of Engineering, Kyoto University, Kyoto 615-8510, Japan

*e-mail: mori@sbchem.kyoto-u.ac.jp

Nature Chemical Biology: doi:10.1038/nchembio.640

Supplementary Methods

Materials. Fura-2 AM ester, 5-nitro-2-pyridyl disulfide (5-nitro-2-PDS), 2-pyridyl disulfide and 1,2-bis(2-aminophenoxy)ethane-*N*,*N*,*N'*,*N'*-tetraacetic acid (BAPTA) were obtained from Dojindo, 2-aminoethyl diphenylborinate (2-APB), capsaicin, N^G-nitro-L-arginine methyl ester (L-NAME), chlorpromazine (CPZ), brefeldin A, dynasore, filipin, edelfosine (ET), bradykinin and pluronic F-127 (F-127) from SIGMA, 4-nitrophenyl disulfide, 4-tolyl disulfide and 4-methoxyphenyl disulfide from Aldrich, 3-nitrophenyl disulfide, phenyl disulfide, diallyl disulfide, dipropyl disulfide, sodium tripolyphosphate, dimethyl sulfoxide (DMSO), glutathione (reduced form) and *N*-acetylcysteine (NAC) from Wako, 4-chlorophenyl disulfide and 4-aminophenyl disulfide from Tokyo Chemical Industry, dimethyloxalylglycine (DMOG) from Frontier Scientific, diphenylene iodonium (DPI) from CALBIOCHEM, DiI from Invitrogen, dithiothreitol (DTT), allyl isothiocyanate (AITC) and 5,5'-dithiobis(2-nitrobenzoic acid) (DTNB) from Nacalai Tesque. DTNB-2Bio was synthesized as previously reported[1]. Compounds such as 5-nitro-2-PDS, 4-nitrophenyl disulfide, 4-tolyl disulfide, 4-methoxyphenyl disulfide, 3-nitrophenyl disulfide, phenyl disulfide, diallyl disulfide, dipropyl disulfide, 4-chlorophenyl disulfide, 4-aminophenyl disulfide, 2-APB, capsaicin, DMOG, AITC, DPI, brefeldin A, CPZ, dynasore, filipin and DTNB were prepared as stock solutions in DMSO and were diluted at working concentrations in aqueous solutions containing 0.01% or 0.1% DMSO. ET was prepared as stock solution in ethanol and was diluted at working concentration in aqueous solutions containing 0.1% ethanol. L-NAME, F-127, NAC, bradykinin, reduced glutathione and DTT were directly dissolved in aqueous solutions at working concentrations.

Nature Chemical Biology: doi:10.1038/nchembio.640

cDNA cloning and plasmid construction. Human TRPA1, TRPV2, PHD1, PHD2 and PHD3 (GenBank accession No. NM007332.1, NM016113, BC036051, NM022051 and NM022073, respectively) were cloned from Human Brain, whole Marathon-Ready cDNA (BD Biosciences) by applying a PCR-based approach designed to contain the untranslated leader sequence from the alfalfa mosaic virus[2] and consensus sequence from the translation initiation[3], and were subcloned into the expression vector pCI-neo (Promega), pEGFP-C (Clontech) and pCMV-tag2 (Stratagene). TRPA1 Cys mutants and Pro mutant were constructed from TRPA1-pCIneo using overlap extension PCR[4]. C414S, C421S, C540S, C621S, C641S and C665S were constructed as previously reported[5]. The primer pairs used for C3S, C59S, C104S, C173S, C192S, C199S, C213S, C258S, C273S, C308S, C462S, C608S, C633S, C651S, C703S, C727S, C773S, C786S, C834S, C856S, C1021S, C1025S, C1085S and P394A are summarized in **Supplementary Table 3**. The double mutant C633S·C856S was generated by digesting C633S-pCIneo with *Xho*I and *Spe*I and inserting this fragment containing the mutation into the *Xho*I and *Spe*I sites of C856S-pCIneo. Catalytically dead PHD1, PHD2 and PHD3 mutants were constructed from PHD1-pCIneo, PHD2-pCIneo and PHD3-pCIneo, respectively, using overlap extension PCR, as previously reported[6–8]. The primer pairs used for PHD1 mutant (H357A), PHD2 mutant (H374A) and PHD3 mutant (H196A) are summarized in **Supplementary Table 3**. The nucleotide sequences of the mutants were verified by sequencing the corresponding cDNA. Plasmids carrying TRPV1, TRPV3, TRPV4, TRPM2, TRPM7, TRPC1, TRPC4 and TRPC5 cDNA were used as previously described[1]. The plasmid vector for the TRP cDNAs was pCI-neo, except pcDNA3.1 (Invitrogen) for TRPV4 cDNA. Functional expression of TRPV2 was confirmed by testing the response to 10 μM

Nature Chemical Biology: doi:10.1038/nchembio.640

L-α-lysophosphatidylcholine[9] (Wako), that of TRPV3 and TRPV4 was confirmed by testing the response to 100 μM 2-APB[10], that of TRPM2 was confirmed by testing the response to 300 μM H_2O_2[11] (Wako), that of TRPC1 and TRPC4 was confirmed by testing the response to 100 μM carbachol[12] (SIGMA) and that of TRPC5 was confirmed by testing the response to 100 μM ATP[13] (SIGMA) in $[Ca^{2+}]_i$ measurement. Functional expression of TRPM7 was confirmed by testing the response to 1 mM Mg^{2+} (ref. 14) in electrophysiological measurement. The plasmid carrying B_2R was a gift from I. Hamachi (Kyoto University).

Synthesis of AP-18 ((*Z*)-4-(4-chlorophenyl)-3-methylbut-3-en-2-oxime)[15–18]. All chemical reagents were purchased from commercial suppliers. Thin layer chromatography (TLC) was performed on silica gel 60 F_{254} precoated aluminum sheets (Merck) and visualized by fluorescence quenching. Chromatographic purification was accomplished using flash column chromatography on silica gel 60 N (neutral, 40–50 μm, Kanto Chemical). Proton nuclear magnetic resonance (^{1}H NMR, 400 MHz) and carbon nuclear magnetic resonance (^{13}C NMR, 100 MHz) spectra were recorded on a Varian MERCURYplus-400 spectrometer with the values given in ppm (Me_4Si, TMS as internal standard) and *J* (Hz) assignments of ^{1}H resonance coupling. Electrospray ionisation in positive mode high resolution mass spectrometry (ESI-HR-MS) spectra were acquired on a Thermo Scientific Exactive mass spectrometer by K. Kuwata (Kyoto University).

In argon atmosphere, a mixture of 3-(acetoxy-(4-chlorophenyl)methyl)-but-3-en-2-one[16,17] (14.0 g, 55.4 mmol), $Pd(OAc)_2$ (0.62 g, 2.77 mmol), 1,2-bis(diphenylphosphino)ethane (DPPE) (3.53 g, 8.86 mmol),

Nature Chemical Biology: doi:10.1038/nchembio.640

formic acid (HCOOH) (6.26 ml, 166 mmol) and triethylamine (NEt_3) (23.0 ml, 166 mmol) in dry THF (300 ml) was refluxed for 3 h. After removal of the solvent, ethyl acetate (200 ml) and hexane (200 ml) were added to the residue. The organic solution was washed with 5% citric acid solution, 10% $NaHCO_3$ solution and brine. The organic layer was dried over $MgSO_4$, and the solvent was evaporated in vacuo. The residue was purified by column chromatography (silica, hexane : ethyl acetate = 8 : 1 → 4 : 1) to give colorless oil. The colorless oil (6.50 g, 33.4 mmol) and hydroxylamine hydrochloride ($NH_2OH{\cdot}HCl$) (3.48, 50.1 mmol) were dissolved in dry ethanol (18 ml) and dry pyridine (36 ml), and were stirred overnight at 60°C. After removal of the solvent, ethyl acetate (150 ml) and hexane (150 ml) were added to the residue. The organic solution was washed with 0.1N HCl solution, 10% $NaHCO_3$ solution and brine. The organic layer was dried over $MgSO_4$, and the solvent was evaporated in vacuo. The residue was purified by recrystallization from ethyl acetate and hexane to afford **AP-18** (6.8 g, 96%) as a white solid. TLC (hexane : AcOEt, 4:1 v/v): R_f = 0.30; ^{1}H-NMR (400 MHz, $CDCl_3$): δ 8.51 (s, 1H), 7.35 (d, 2H, *J* = 8.4 Hz), 7.25 (d, 2H, *J* = 8.4 Hz), 6.85 (s, 1H), 2.16 (s, 3H), 2.05 (s, 3H); ^{13}C-NMR (100 MHz, $CDCl_3$): δ 158.4, 135.8, 135.5, 133.1, 130.8, 129.9, 128.6, 14.4, 10.5; HR-MS (*m/z*): $[M+H]^+$ calcd. for $C_{11}H_{13}ClNO$, 210.0680; found, 210.0675.

AP-18 was prepared as stock solutions in DMSO and was diluted at working concentrations in aqueous solutions containing 0.01% DMSO.

Measurement of changes in $[Ca^{2+}]_i$. The fura-2 fluorescence was measured in HEPES-buffered saline (HBS) containing the following (in mM): 107 NaCl, 6 KCl, 1.2 $MgSO_4$, 2 $CaCl_2$, 11.5 glucose and 20 HEPES (pH adjusted to 7.4 with NaOH). For

Nature Chemical Biology: doi:10.1038/nchembio.640

Supplementary Figure 9a, **Supplementary Figure 21e,f** and **Supplementary Figure 22g,h**, the fura-2 fluorescence was measured in bicarbonate/CO_2 buffered solution containing following (in mM): 124.8 NaCl, 5 KCl, 1.2 KH_2PO_4, 1.3 $MgSO_4$, 2 $CaCl_2$, 24 $NaHCO_3$ and 10 glucose (pH adjusted to 7.4 with 5% CO_2-bubbling). Fluorescence images of the cells were recorded and analyzed with a video image analysis system (AQUACOSMOS; Hamamatsu Photonics) according to the manufacturer's instructions. The 340:380-nm ratio images were obtained on a pixel-by-pixel basis. Fura-2 measurements were carried out at 21 ± 1°C in HBS. The 340:380-nm ratio images were converted to Ca^{2+} concentrations by *in vivo* calibration using 5 μM ionomycin as described previously[5]. Hyperoxic solution was achieved by bubbling with 22, 24, 26, 28, 30, 32, 34, 36, 80, 95 or 100% O_2 (balanced with N_2) gas for at least 20 min before cell perfusion. Hypoxic solution was achieved by bubbling with 0, 5, 8, 10, 12, 14, 16 or 18% O_2 (balanced with N_2) gas at least 20 min before cell perfusion and by blowing the respective gas over the surface of the experimental chamber using a modified dish. The concentration of dissolved O_2 in the chamber solution was determined with an O_2 microelectrode (InLab 605; METTLER TOLEDO). pH of 7.4 was maintained in the buffers after bubbling with N_2 and/or O_2 gas. Unless otherwise indicated, dissolved PO_2 measured in hypoxic, normoxic and hyperoxic solutions were 10% O_2, 20% O_2 and 86% O_2, respectively.

Electrophysiology. For electrophysiological measurements, coverslips with cells were placed in dishes containing the solutions. Currents from cells were recorded at room temperature (22–25°C) using patch-clamp techniques of whole-cell mode, cell-attached mode, excised outside-out mode and excised inside-out mode, with EPC-9 (Heka

Nature Chemical Biology: doi:10.1038/nchembio.640

Electronic) or Axopatch 200B (Molecular devices) patch-clamp amplifier as previously described[19]. The patch electrodes prepared from borosilicate glass capillaries had a resistance of 2–4 MΩ for whole cell recordings and 5–7 MΩ for single-channel recordings. Current signals were filtered at 5 kHz with a four-pole Bessel filter and digitized at 10 or 20 kHz. PULSE (version 8.8; Heka Electronic) or pCLAMP (version 10.0.2; Molecular devices) software was used for command pulse control, data acquisition and analysis. For whole cell recordings, series resistance was compensated (to 70–80%) to minimize voltage errors. Ramp pulses were applied every 5 or 10 sec from –100 mV to +100 mV or from +100 mV to –100 mV at a speed of 1.1 mV ms^{-1} from a holding potential (V_h) of 0 mV. The extracellular (bath) solution contained the following (in mM): 100 NaCl, 2 Ca-gluconate and 10 HEPES (pH 7.4 adjusted with NaOH, and osmolality adjusted to 320 mmol kg^{-1} with D-mannitol). Intracellular (pipette) solution contained the following (in mM): 100 Cs-aspartate, 5 BAPTA, 1.4 Ca-gluconate, 2 Na_2ATP, 2 $MgSO_4$, 1 $MgCl_2$, 10 HEPES and 10 $Na_5P_3O_{10}$ (pH 7.4 adjusted with CsOH, and osmolality adjusted to 320 mmol kg^{-1} with D-mannitol). The free Ca^{2+} concentration was 30 nM calculated with CaBuf software (provided by Dr. Droogmans, G., Katholieke Universiteit Leuven, Leuven, Belgium). For **Supplementary Figure 4d,e**, Ca-gluconate was omitted from bath solution and added 5 mM EGTA. For **Figure 5b–d,h**, **Supplementary Figure 13b** and **Supplementary Figure 17a–d**, pipette solution contained the following (in mM): 50 Cs-aspartate, 50 CsCl, 10 $Na_5P_3O_{10}$, 0.3 2-oxoglutarate, 0.1 $FeCl_2$, 3 ascorbic acid and 10 HEPES in the presence or absence of 0.67 μM purified PHD2 (pH 7.4 adjusted with CsOH, and osmolality adjusted to 300 mmol kg^{-1} with D-mannitol). For the recording of nodose ganglion neurons, Ca-gluconate was omitted from pipette solution. Percentage

Nature Chemical Biology: doi:10.1038/nchembio.640

suppression of the current (%) in **Supplementary Figure 2b**, **Supplementary Figure 9f** and **Supplementary Figure 21g,h** were calculated according to the following equation; percentage suppression of the current (%) = $100\times(1 - I_A/I_{Ctl})$, where I_{Ctl} and I_A are whole cell currents observed before and after application of agents. Percentage increment of the current (%) in **Figure 5d**,**h** and **Supplementary Figure 13b** were calculated according to the following equation; percentage increment of the current (%) = $100\times(I_A/I_{Ctl} - 1)$, where I_{Ctl} and I_A are whole cell currents observed before and after application of agents. Single-channel recordings were performed in cell-attached and in inside-out and outside-out excised patches configuration. Single-channel events were detected using the 50% threshold detection method. From the single-channel events list, histograms of channel open dwell time distributions were plotted and fitted using a maximum likelihood procedure with correction for missed events. The minimal number of exponential components required to fit the distribution was determined by chi-square statistics. Mean open durations were calculated, from the open dwell time fitted components, as a weighted mean from the open durations and proportions of each component. The NP_O of single-channels was calculated by dividing the total time spent in the open state by the total time of continuous recording (30 sec) in the patches containing active channels. The amplitude of single-channel currents was measured as the peak-to-peak distance in Gaussian fits of the amplitude histogram. Activity plots of NP_O recorded from cell-attached patches, as calculated for a 5-sec to V_h of 60 mV, and plotted as a vertical bar on the activity histogram. For cell-attached recordings, the pipette solution contained the following (in mM): 100 CsCl, 1 $MgCl_2$, 1 EGTA and 10 HEPES (pH 7.4 adjusted with CsOH, and osmolality adjusted to 300 mmol kg^{-1} with D-mannitol). For **Supplementary Figure 3h**,**i** and

Nature Chemical Biology: doi:10.1038/nchembio.640

Supplementary Figure 4a, the extracellular side was exposed to a bath solution containing (in mM) 140 NaCl, 5 KCl, 2 $CaCl_2$, 1 $MgCl_2$, 10 HEPES and 10 glucose (pH 7.4 adjusted with NaOH, and osmolality adjusted to 300 mmol kg^{-1} with D-mannitol). For **Supplementary Figure 17e,f**, the extracellular side was exposed to a bath solution containing (in mM) 5 NaCl, 140 KCl, 1 $MgCl_2$, 5 EGTA, 10 HEPES and 10 glucose (pH 7.4 adjusted with NaOH, and osmolality adjusted to 300 mmol kg^{-1} with D-mannitol). For inside-out patch recordings, the pipette solution contained the following (in mM): 100 CsCl, 1 $MgCl_2$, 1 EGTA and 10 HEPES (pH 7.4 adjusted with CsOH, and osmolality adjusted to 300 mmol kg^{-1} with D-mannitol). The intracellular side was exposed to bath solution containing the following (in mM): 50 Cs-aspartate, 50 CsCl, 1 $MgCl_2$, 1 $CaCl_2$, 10 EGTA, 10 $Na_5P_3O_{10}$ and 10 HEPES (pH 7.4 adjusted with CsOH, and osmolality adjusted to 300 mmol kg^{-1} with D-mannitol). For **Figure 2f,g** and **Supplementary Figure 3g,j**, concentration of $Na_5P_3O_{10}$ was reduced from 10 to 1 mM. For outside-out patch recordings, the intracellular and the bath solution were identical to that used for whole cell recordings. Percentage suppression of the NP_O (%) in **Figure 2f,g** and **Supplementary Figure 3d** were calculated according to the following equation; percentage supression of the NP_O (%) = $100\times(1 - NP_{O\,A}/NP_{O\,Ctl})$, where $NP_{O\,Ctl}$ and $NP_{O\,A}$ indicate mean NP_O of 60 sec obtained before and 4-min after application of 10 μM AP-18 or 10 mM DTT. pH of 7.4 was maintained in the buffers after bubbling with N_2 and/or O_2 gas. Unless otherwise indicated, dissolved PO_2 measured in hypoxic, normoxic and hyperoxic solutions were 10% O_2, 20% O_2 and 86% O_2, respectively.

DTNB-2Bio labeling assay. The DTNB-2Bio labeling assay was performed as

Nature Chemical Biology: doi:10.1038/nchembio.640

previously described with modifications[1]. HEK293 cells (~5×10^6) transfected with GFP-TRPA1 (GFP-WT), GFP-C633S, GFP-C856S or vector were washed with phosphate-buffered saline (PBS). The surface membrane was permeabilized by exposure to PBS containing 0.001% digitonin (SIGMA) for 5 min. The cells were collected and incubated in HBS solution containing 50 μM DTNB-2Bio for 20 min at room temperature. The cells were washed with HBS and lysed in RIPA buffer (pH 8.0) containing 150 mM NaCl, 1% Nonidet P-40, 0.5% sodium deoxycholate, 0.1% SDS and 50 mM Tris. Cell lysates were incubated batch-wise with NeutrAvidin-Plus beads (Thermo Scientific) for 4 h at 4°C with constant shaking. The beads were rinsed three times with RIPA buffer by centrifugation at 15,000 rpm for 1 min. The proteins were eluted in RIPA buffer containing 50 mM DTT for 1 h and denatured in SDS sample buffer containing 50 mM DTT for 30 min at room temperature. The proteins were analyzed by 7.5% SDS-PAGE and WB using an antibody to GFP (Clontech).

Expression and purification of recombinant PHD2. HEK293T cells were transfected with PHD2-pCMV-tag2 using Lipofectamine 2000 in 100-mm tissue culture dishes. Thirty-six hour after transfection, the cells from 20 dishes were washed with PBS and lysed in 10 ml of Triton buffer (pH 7.5) containing 50 mM Tris, 150 mM NaCl, 0.1% Triton X-100 and protease inhibitors. After centrifugation for 15 min at 17,000 *g*, the supernatant containing Flag-tagged PHD2 was loaded onto 1 ml of anti-Flag affinity gel column (SIGMA), equilibrated in advance. After washing the column with 5 ml of Triton buffer and 15 ml of Tris-buffered saline (TBS) (pH 7.5) containing 50 mM Tris and 150 mM NaCl, the bound protein was eluted with 3 ml of elution buffer (300 μg ml^{-1} Flag peptide (SIGMA) in TBS buffer). The eluate was concentrated to 300 μl,

Nature Chemical Biology: doi:10.1038/nchembio.640

and the buffer was exchanged simultaneously into Cs buffer (pH 7.4 adjusted with CsOH) containing 50 mM CsCl, 50 mM CsOH, 50 mM L-aspartic acid and 10 mM HEPES using Amicon Ultra-4 centrifugal filter units (30-kDa cut-off) (Millipore).

Coimmunoprecipitation in HEK293 cells. Forty eight hour after transfection, HEK293 cells were lysed in RIPA buffer. The cell lysate was immunoprecipitated with M2 monoclonal antibody to Flag (SIGMA) or monoclonal antibody to glutathione (VIROGEN) in the presence of protein A-sepharose beads (GE Healthcare) by rocking for 4 h at 4^{o}C. The immune complexes were washed three times with RIPA buffer and resuspended in SDS sample buffer containing 50 mM DTT for 30 min at room temperature. The proteins were analyzed by 7.5% SDS-PAGE and WB using antibody to GFP (Clontech), polyclonal antibody to Flag (SIGMA) or antibody to TRPA1(hydroxylated Pro394) raised against the peptide containing LKNLRP(OH)EFMQ (SIGMA). For **Figure 4d**, **Supplementary Figure 10e** and **Supplementary Figure 14b**, the cells were pretreated with 1 mM DMOG for 48 h to stabilize the enzyme-substrate interaction[20]. Dissolved PO_2 measured in hypoxic, normoxic and hyperoxic solutions were 10% O_2, 20% O_2 and 86% O_2, respectively.

TIRF microscopy. TIRF images were acquired using a TIRF illumination system (IX2-RFAEVA-2, Olympus) mounted on an inverted microscope equipped with an autofocus system (IX81-ZDC2, Olympus). A diode-pumped solid state 488-nm laser (kyma488, 10 milliwatts, MELLES GRIOT) was used for total fluorescence illumation, and a 510-nm long pass filter was used as an emission filter. Images were captured by a high-sensitivity EM-CCD camera (ImagEM, Hamamatsu Photonics) operated with

Nature Chemical Biology: doi:10.1038/nchembio.640

MetaFluor software (Molecular Devices). HEK293 cells transfected with GFP-TRPA1 were plated onto poly-L-lysine-coated glass coverslips (Iwaki) and were placed in a custom chamber with HBS solution at room temperature. Prior to the addition of any agents, cells were first imaged for 2 min to establish the base line. For fluorescence intensity analysis, regions of interest with areas between 5–10% of the visible footprint of individual cells were drawn. Data are presented as the ratio of the fluorescence intensity at each point divided by the fluorescence intensity at the start of the experiment (F/F_0), where each value was background-subtracted to correct for the dark-field noise of the camera. Images were captured every 10 sec. Dissolved PO_2 measured in hypoxic and normoxic solutions were 10% O_2 and 20% O_2, respectively.

siRNA suppression of endogenous PHDs in HEK293 cells. The sense siRNA sequences 5'-AACCAGGCTGTCGAAGCATTG-3', 5'-AACATCGAGCCACTCTTTGAC-3' and 5'-AAGGTGTCCAAGTACCTGTAT-3' for PHD1, 5'-AACAAGCACGGCATCTGTGTG-3', 5'-AAGGACATCCGAGGCGATAAG-3' and 5'-AAGGTAAGTGGAGGTATACTT-3' for PHD2 and 5'-AAGGAGAGGTCTAAGGCAATG-3', 5'-AACAGGTTATGTTCGCCACGT-3' and 5'-AACGGTGATGGTCGCTGCATC-3' for PHD3 were used. To construct siRNA oligomers, the Silencer siRNA construction kit (Ambion) was used. The GAPDH siRNA used was the control provided with the kit. Transfection of siRNAs to HEK293 cells was carried out using Lipofectamine 2000 (Invitrogen). Cells were transfected with total 200 pmol siRNA in a 60-mm culture dish. Total RNA was extracted using ISOGEN (Wako), following the manufacturer's instructions. The concentration and purity of RNA were determined

Nature Chemical Biology: doi:10.1038/nchembio.640

spectrophotometrically. Suppression of RNA expression was confirmed by RT-PCR analyses (30 cycles) using specific primers listed in **Supplementary Table 4**. RT-PCR was performed using the LA-PCR kit (TaKaRa), according to the manufacturer's instructions. The cells treated with siRNAs were subjected to $[Ca^{2+}]_i$ measurement 36–48 h after transfection.

Cell surface labeling experiment. The cell surface GFP-TRPA1 was measured by biotinylation as previously described[1] with modifications. The cells were preincubated with 200 μM brefeldin A (for **Supplementary Figure 18h**) or 5 μg ml^{-1} CPZ (for **Supplementary Figure 18i**) for 3–4 h, and then were washed with PBS. After incubation in normoxic or hypoxic HBS solution for 5 min, the cells were incubated with 0.5 mg ml^{-1} Sulfo-NHS-SS-Biotin (Thermo Scientific) in normoxic or hypoxic HBS solution for 5 min at room temperature. The cells were washed with PBS containing 100 mM glycine three times to stop the biotinylation reaction and to remove free biotin. The cells were then lysed in RIPA buffer. After centrifugation, the supernatant was collected and incubated with streptavidin-agarose beads (Thermo Scientific) overnight at 4°C. The samples were washed with RIPA buffer six times. The proteins were eluted in RIPA buffer containing 50 mM DTT for 1 h and denatured in SDS sample buffer containing 50 mM DTT for 30 min at room temperature. The proteins were analyzed by 7.5% SDS-PAGE and WB using an antibody to GFP (Clontech). Dissolved PO_2 measured in hypoxic and normoxic solution were 10% O_2 and 20% O_2, respectively.

Mice. Mice were housed in a standard environmental condition (12-h light/12-h dark

Nature Chemical Biology: doi:10.1038/nchembio.640

cycle; about 23°C). All experimental procedures were performed in accordance with the National Institute of Health Guide for the Care and Use of Laboratory Animals and approved by the Institutional Animal Use Committees of Kyoto University and Kagoshima University. Experiments were performed using C57BL/6J, 129S6, *Trpa1* KO, *Phd1* KO and *Phd3* KO mice. C57BL/6J mice were used as nontransgenic controls for *Trpa1* KO mice, while 129S6 mice were used as nontransgenic controls for *Phd1* KO and *Phd3* KO mice. *Trpa1* KO mice were purchased from the Jackson Laboratory and genotyped as previously described[21]. *Phd1* KO and *Phd3* KO mice were derived as previously described[22,23].

Coimmunoprecipitation of endogenous TRPA1 with PHD2 proteins. Mouse DRG was lysed in RIPA buffer and the cell extract was immunoprecipitated with antibody to PHD2 (Novus Biologicals) in the presence of protein A-sepharose beads (GE Healthcare) by rocking for 4 h at 4^{o}C. The immune complexes were washed three times with RIPA buffer and resuspended in SDS sample buffer containing 50 mM DTT for 2 h at room temperature. The proteins were analyzed by 7.5% SDS-PAGE and WB using an antibody to TRPA1, which was a gift from Y. Kubo[24].

RNA isolation and RT-PCR in mouse nodose ganglion or DRG neurons. Total RNA was extracted using ISOGENE, following the manufacturer's instructions. The concentration and purity of RNA were determined spectrophotometrically. Two hundred nanograms of total RNA were reverse-transcribed into first-strand cDNA by use of the RNA LA PCR kit at the final volume of 20 µl. Expression levels of PHD1–3 RNA in mouse nodose ganglion or DRG neurons were determined by RT-PCR. The

Nature Chemical Biology: doi:10.1038/nchembio.640

primers used for PCR amplification are summarized in **Supplementary Table 4**. PCR was conducted with a GeneAmp PCR system 9700 (Applied Biosystems) using LA Taq polymerase with GC buffer (TaKaRa) for 32 cycles under the following conditions: initial denaturation was 3 min at 95°C, then 30 sec at 95°C, following by a 30-sec annealing step at 55°C and 30-sec elongation at 72°C, and a final elongation of 7 min at 72°C. Predicted lengths of PCR products are 543, 388 and 468 base pairs (bp) for PHD1, PHD2 and PHD3, respectively.

Immunohistochemistry of airway- and lung-identified nodose ganglion neurons and DRG neurons. For immunohistochemistry of airway- and lung-identified nodose ganglion neurons, WT mice were anaesthetized with pentobarbital (50 mg kg^{-1}). To label neurons that project fibres into the trachea, mice were orotracheally intubated, and 50 μl of the tracer DiI (dissolved in 100% ethanol and diluted in sterile saline to a final concentration of 0.5 mg ml^{-1} in 1% ethanol) was instilled into the tracheal lumen. On the other hand, in order to label neurons that project fibres deep into the lung, mice were transdermally injected with 50 μl of DiI (0.5 mg ml^{-1}) into the right lung. Eight days after injection, the mice were killed by an overdose of pentobarbital (150 mg kg^{-1}). The nodose ganglions were removed from the mice without perfusion of fixation solution. The samples were then rinsed with PBS, embedded in OCT compound (Sakura Finetek) and 'snap-frozen' in dry ice and acetone and stored at –80°C. Cryostat sections (3 μm in thickness) were affixed to micro slides (MATSUNAMI), dried at room temperature, fixed in cold acetone for 10 min and then dried at room temperature. The samples were rehydrated in TBS, pH 7.6, and blocked with 1% bovine serum albumin (BSA) and 5% normal goat serum (NGS) in TBS for 1 h at room

Nature Chemical Biology: doi:10.1038/nchembio.640

temperature. The samples were incubated with anti-mouse TRPA1 antibody[24] as a primary antibody overnight at 4°C, washed with 1% BSA and 5% NGS in TBS at room temperature and then incubated with Alexa Fluor 488-conjugated goat anti-rabbit IgG (Invitrogen) as a secondary antibody for 2 h at 4°C. Followed by washing with 1% BSA and 5% NGS in TBS, the coverslips were sealed with PermaFluor Aqueous (IMMUNONTM, SHANDON) to prevent evaporation and stored at 4°C before imaging.

For immunohistochemistry of DRG neurons, 18 h after of DRG isolation, the neurons were fixed with 4% paraformaldehyde and then permeabilized with 0.1% Triton X-100. The neurons were incubated with anti-mouse TRPA1 antibody[24] followed by incubation with Alexa Fluor 488-conjugated goat anti-rabbit IgG (Invitrogen). Thereafter the neurons were incubated with rabbit IgG to mask the residual reactivity of Alexa Fluor 488-conjugated goat anti-rabbit IgG, and then incubated with Alexa Fluor 546 (Invitrogen)-conjugated anti-TRPA1(hydroxylated Pro394) which was prepared as previously described[25].

The fluorescence images were acquired with a confocal laser-scanning microscope using the 488-nm line of an argon laser for excitation and a 505–525 nm band-pass filter for emission and 543-nm line of a He-Ne laser for excitation and a 560-nm long-pass filter for emission. The specimens were viewed at high magnification using plan oil objectives (60×, 1.40 NA, Olympus).

Semi-quantitative RT-PCR analysis of PHD1–3. Expression levels of PHD1–3 RNA in mouse DRG or nodose ganglion neurons were compared by semi-quantitative RT-PCR. The primers used for PCR amplification are summarized in **Supplementary**

Nature Chemical Biology: doi:10.1038/nchembio.640

Table 4. PCR was conducted under the following conditions: 94°C for 5 min followed by 30 cycles for PHD1 and PHD2 or 32 cycles for PHD3 at 94°C for 30 sec, 55°C for 30 sec and 72°C for 40 sec, and finally 72°C for 7 min. Predicted lengths of PCR products are 543, 388 and 468 bp for PHD1, PHD2 and PHD3, respectively. Plasmids carrying PHD1, PHD2 or PHD3 cDNA were used as control.

siRNA suppression of endogenous PHDs in DRG neurons. Freshly isolated DRG neurons were nucleofected with siRNAs using the Basic Neuron SCN Nucleofector kit and SCN Basic Neuro Program 6 (Amaxa) according to manufacturer's protocol. The siRNA for directed to PHD1 (ON-TARGETplus SMARTPool, L-051750), PHD2 (ON-TARGETplus SMARTPool, L-040757), PHD3 (ON-TARGETplus SMARTPool, L-040261) and negative control siRNA (ON-TARGETplus Non-targeting siRNA, D-001810) were purchased from Dharmacon. Nucleofected DRG neurons were plated on 24 well culture dish coated with poly-L-lysine and laminin. Total RNA was extracted using NucleoSpin RNA XS (Macherey-Nagel) 36 h after transfection, following the manufacturer's instructions. The concentration and purity of RNA were determined spectrophotometrically. Suppression of RNA expression was confirmed by RT-PCR analyses (32 cycles) using specific primers listed in **Supplementary Table 4**. RT-PCR was performed using the LA-PCR kit, according to the manufacturer's instructions. The cells treated with siRNAs were subjected to $[Ca^{2+}]_i$ measurement 36–48 h after transfection. In $[Ca^{2+}]_i$ measurement, siRNAs were cotransfected with pEGFP-F, and neurons with green fluorescence were analyzed.

Recording of multifiber vagal and superior laryngeal afferent discharges. WT or

Nature Chemical Biology: doi:10.1038/nchembio.640

Trpa1 KO mouse was anesthetized with intraperitoneal injection of urethane. L-shaped cannula perforated at the corner was inserted to the trachea. The animal was then artificially ventilated with room air and paralyzed with 0.15 mg kg^{-1} panchronium bromide. Acute unilateral nerve sectioning was performed as follows: right cervical vagal trunk was exposed and cut immediately below the point of branching off to the superior laryngeal nerve; right superior laryngeal nerve was exposed and cut. To record the afferent activities, the distal cut end was placed on a pair of silver hook electrodes. Multifiber vagal and superior laryngeal nerve discharges were amplified (10,000×, AVB-8, Nihon Kohden) and displayed on an oscilloscope (5113, Tektronix, Beaverton). The lower and higher cut-off frequencies of the recording system were 100 and 3,000 Hz, respectively. Nerve discharges were full-wave rectified, leaky integrated (time constant = 1 sec, EI-601G, Nihon Kohden) and stored in a hard disk through an analog-to-digital converter (PowerLab, ADInstrument) together with original nerve discharges, electrocardiogram, inspired PO_2 and PCO_2 and the event signal. At the end of each experiment, the vagal or superior laryngeal nerve was cut proximally to the recording electrode and the mean level of instrumentation noise was determined over the period of several minutes. At the time of reproduction, rectified and integrated vagal or superior laryngeal nerve activity was subtracted by this noise level to obtain each nerve activity. During the control period, the animal was breathed room air. The animal was then challenged with five levels of inspired O_2 (10, 13, 15, 20 and 100% O_2). Normoxic and hyperoxic gas challenges lasted 35 sec, and hypoxic challenge lasted 25 sec, respectively. The order of applied gas conditions was chosen randomly for each experiment, and gas challenge was followed by a 5-min interval in room air. Throughout the experiment, rectal temperature was kept constant at 36.5 ±

Nature Chemical Biology: doi:10.1038/nchembio.640

1.0°C by a heating pad connected to a thermo controller.

Nature Chemical Biology: doi:10.1038/nchembio.640

Supplementary Results

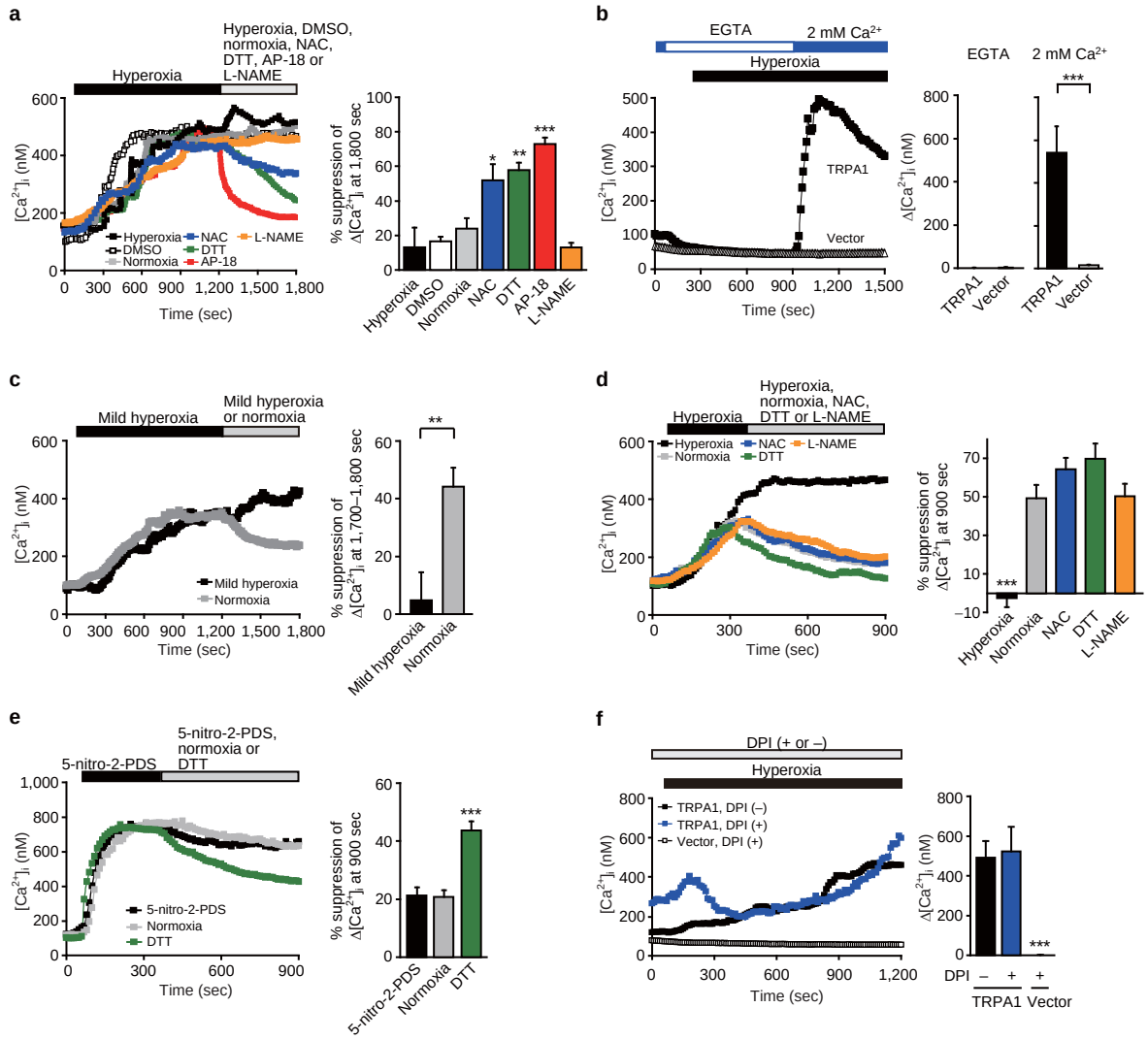

Supplementary Figure 1. Pharmacological characterization of hyperoxia-activated TRPA1 responses. (**a**) TRPA1 responses evoked by the 19-min treatment with hyperoxic solution are sustained after switching the condition to normoxia alone or in combination with vehicle for AP-18 (0.01% DMSO) or 300 μM L-NAME but are suppressed after switching the condition to normoxia in conbination with 1 mM NAC, 1 mM DTT or 10 μM AP-18 in HEK293 cells. Averaged time courses and percentage suppression of $[Ca^{2+}]_i$ rises at 1,800 sec relative to maximum $[Ca^{2+}]_i$ rises ($\Delta[Ca^{2+}]_i$) up to 1,200 sec (n = 18–26). $^{*}P < 0.05$, $^{**}P < 0.01$ and $^{***}P < 0.001$ compared to cells treated with normoxic solution. (**b**) Averaged time courses and $\Delta[Ca^{2+}]_i$ induced by hyperoxia (n = 11–28) in Ca^{2+}-free, 0.5 mM EGTA- or 2 mM Ca^{2+}-containing solution are shown for HEK293 cells transfected with TRPA1 or vector. $^{***}P <$ 0.001. (**c**) TRPA1 responses evoked by the 19-min treatment with mild hyperoxic solution are suppressed by normoxic solution in HEK293 cells. Averaged time courses and percentage suppression of average $[Ca^{2+}]_i$ rises at 1,700–1,800 sec relative to $\Delta[Ca^{2+}]_i$ up to 1,200 sec (n = 20–21). Dissolved PO_2 measured in mild hyperoxic solution is 209 mmHg (28% O_2). $^{**}P < 0.01$. (**d**) TRPA1 responses evoked by the 5-min treatment with hyperoxic solution are suppressed after switching the condition to normoxia alone or in combination with 1 mM NAC, 1 mM DTT or 300 μM L-NAME in HEK293 cells. Averaged time courses and percentage suppression of $[Ca^{2+}]_i$ rises at 900 sec relative to $\Delta[Ca^{2+}]_i$ up to 360 sec (n = 13–20). $^{***}P < 0.001$ compared to cells treated with normoxic solution. (**e**) TRPA1 responses evoked by the 5-min treatment with 10 μM 5-nitro-2-PDS are suppressed by 1 mM DTT, but not by normoxic solution in HEK293 cells. Averaged time courses and percentage suppression of $[Ca^{2+}]_i$ rises at 900 sec relative to $\Delta[Ca^{2+}]_i$ up to 360 sec (n = 19–25). $^{***}P < 0.001$ compared to cells maintained with 5-nitro-2-PDS. (**f**) DPI fails to suppress the response of TRPA1 to hyperoxia. Effect of 10 μM DPI on TRPA1 responses evoked by hyperoxia. Thirty-min prior to the treatment with hyperoxic solution and continuing during the treatment, cells are incubated with DPI or its vehicle (0.01% DMSO). Averaged time courses and $\Delta[Ca^{2+}]_i$ (n = 19–28). $^{***}P < 0.001$ compared to TRPA1-expressing HEK293 cells treated with hyperoxic solution without DPI. Data points are mean ± s.e.m..

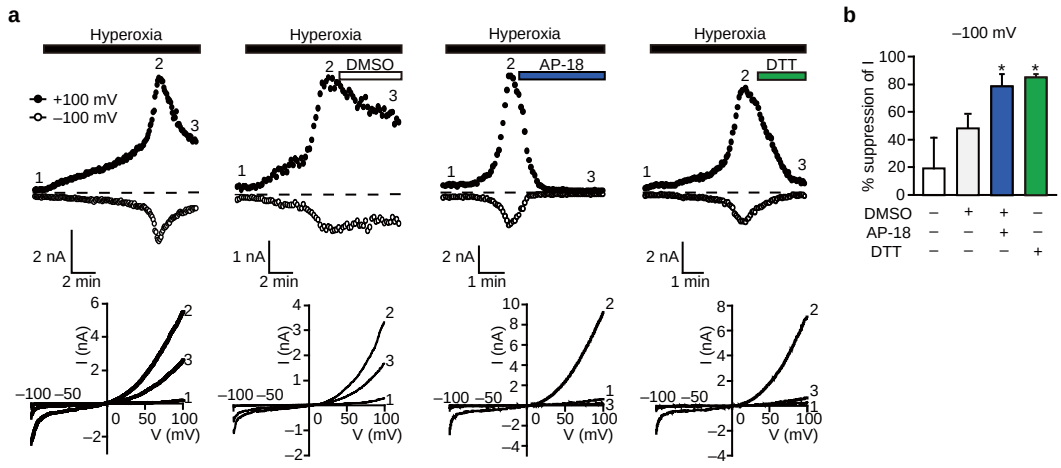

Supplementary Figure 2. Electrophysiological and pharmacological characterization of hyperoxia-activated TRPA1 whole cell currents. (**a**) Suppression of hyperoxia-evoked whole cell currents by vehicle for AP-18 (0.01% DMSO), 10 μM AP-18 and 10 mM DTT in TRPA1-expressing HEK293T cells. Representative time courses of outward and inward currents recorded at +100 and –100 mV, respectively, under ramp clamp. Corresponding *I-V* relationships at the time points 1–3. (**b**) Percentage suppression of the suppressed current (2–3) at 2-min after the peak relative to the induced current at the peak (2–1). (n = 5–7) at –100 mV. $^{*}P < 0.05$ compared to cells maintained in hyperoxia without the agents. Data points are mean ± s.e.m..

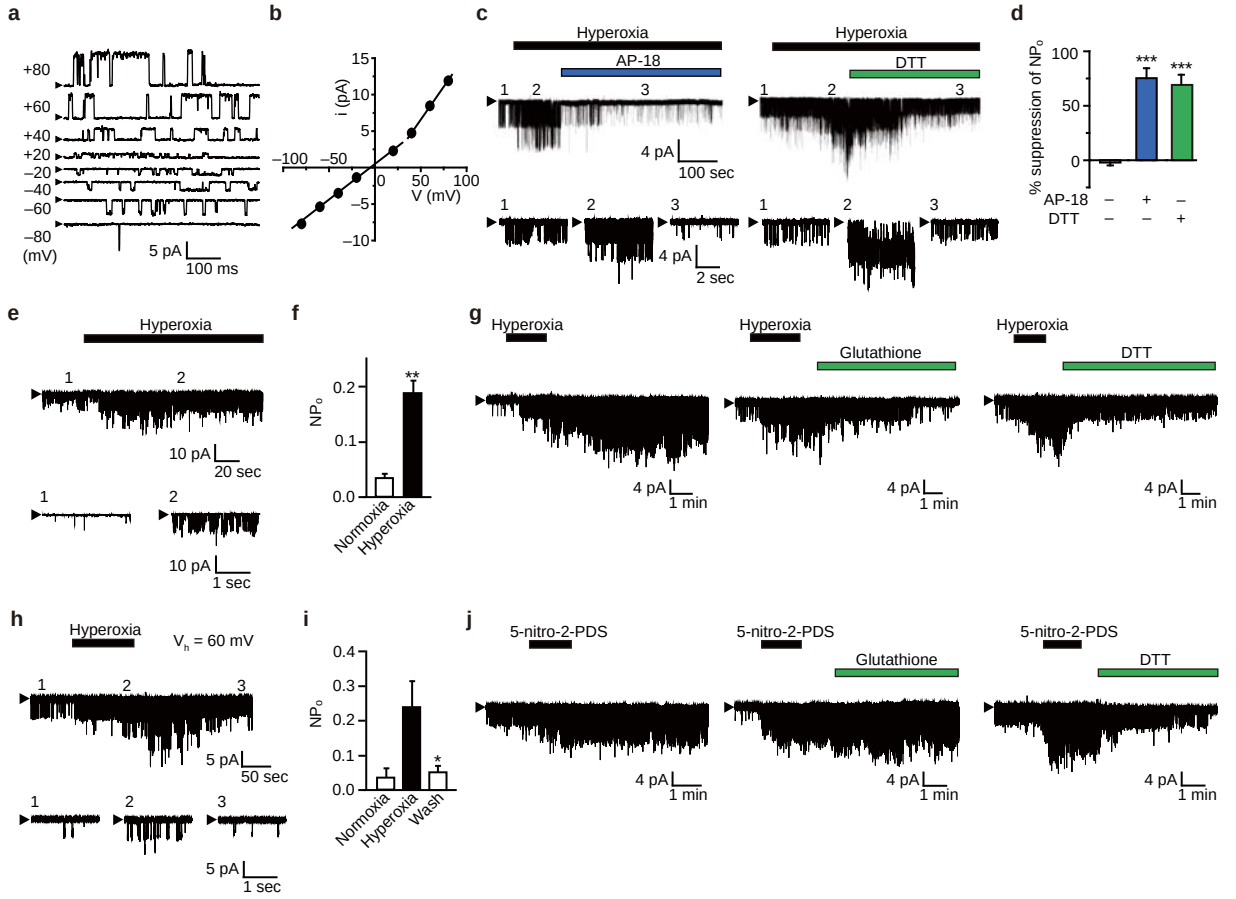

Supplementary Figure 3. Electrophysiological and pharmacological characterization of hyperoxia-activated TRPA1 single channel currents. (**a–j**) Single channel TRPA1 currents from inside-out patches (**a–d,g,j**), outside-out patches (**e,f**) and cell-attached patches (**h,i**). In (**a**), representative current traces of single TRPA1 channel evoked by hyperoxia at different voltages in inside-out patches excised from TRPA1-expressing HEK293T cells are shown. Arrowheads represent the closed state. In (**b**), current-voltage (*i-V*) relationship for unitary currents is shown (n = 5–8). In (**c**), suppression of hyperoxia-evoked single channel currents by AP-18 and DTT at –60 mV in inside-out patches excised from HEK293T cells expressing TRPA1 is shown. Time-expanded current traces in normoxia (trace 1) and in hyperoxia without (trace 2) and with the agents (trace 3) are shown in the bottom panels. In (**d**), percentage suppression of hyperoxia-induced NP_O in control (n = 29) and after 5-min application of AP-18 (n = 8) or DTT (n = 11) is shown. $^{***}P < 0.001$ compared to cells maintained in hyperoxia without the agents. In (**e**), single channel activities evoked by application of hyperoxic solutions at –60 mV in outside-out patches excised from HEK293 cells transfected with TRPA1 are shown. Time-expanded current traces before (trace 1) and during (trace 2) application are also shown in the bottom panels. In (**f**), averages of NP_O representing single TRPA1 channel activity in normoxia (n = 6) and hyperoxia (n = 6) are shown. $^{**}P < 0.01$. In (**g**), suppression of hyperoxia-evoked single channel currents by 5 mM reduced glutathione and 10 mM DTT at –60 mV in inside-out patches excised from HEK293 cells expressing TRPA1 are shown. Percentage suppression of hyperoxia-induced NP_O is shown in **Figure 2f**. In (**h**), single channel activities evoked by application of hyperoxic solutions at V_h of 60 mV in cell-attached patches from HEK293 cells transfected with TRPA1 are shown. Time-expanded current traces before (trace 1), during (trace 2) and after (trace 3) exposure to hyperoxic solution are also shown in the bottom panels. In (**i**), averages of NP_O show single TRPA1 channel activity before, during, and after 4-min exposure to hyperoxic solution (n = 7) are shown. $^{*}P < 0.05$ compared to cells maintained in hyperoxia. In (**j**), suppression of 10 μM 5-nitro-2-PDS-evoked single channel currents by 5 mM reduced glutathione and 10 mM DTT at –60 mV in inside-out patches excised from HEK293 cells expressing TRPA1 are shown. Percentage suppression of 5-nitro-2-PDS-induced NP_O is shown in **Figure 2g**. Data points are mean ± s.e.m..

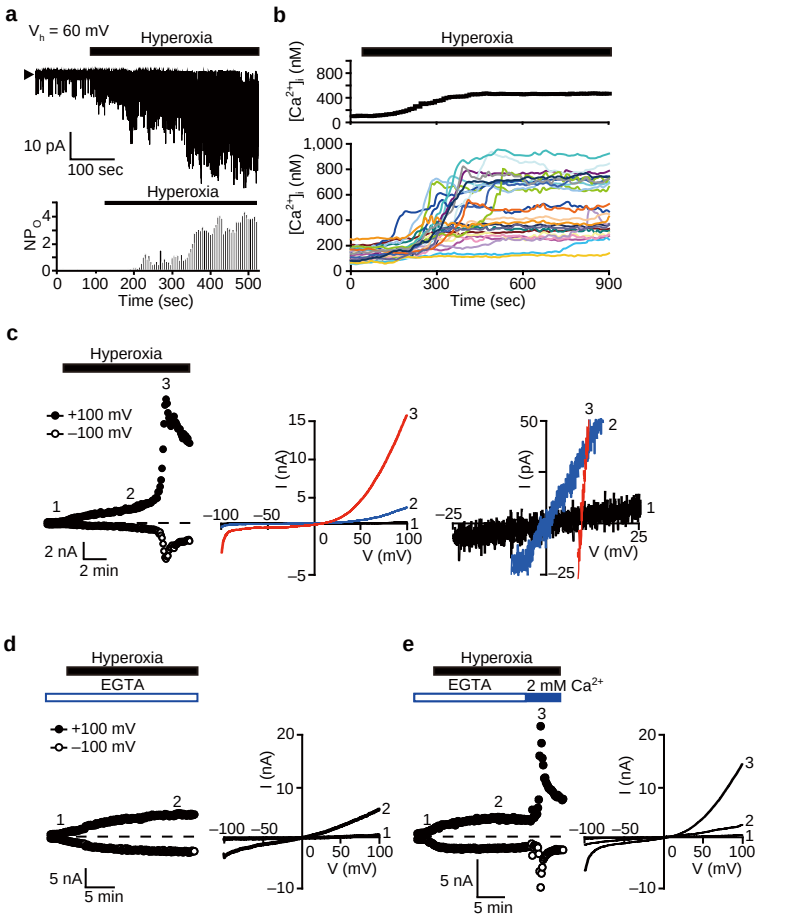

Supplementary Figure 4. Activation patterns of ionic current and Ca^{2+} responses in response to hyperoxia. (**a**) Single channel activities evoked by application of hyperoxic solution at V_h of 60 mV in cell-attached patches from HEK293 cells transfected with TRPA1. Representative current trace and open probability histogram. An arrowhead represents the closed state. Bin width for the histograms is 5 sec. (**b**) TRPA1 channels show a characteristic time course in $[Ca^{2+}]_i$ and electrophysiological measurements. Averaged time courses of $[Ca^{2+}]_i$ changes and the corresponding raw data in TRPA1-expressing HEK293 cells (n = 25). (**c**) Representative time courses of outward and inward whole cell currents recorded at +100 and –100 mV, respectively, under ramp clamp in hyperoxic solution in HEK293T cells transfected with TRPA1. Corresponding *I-V* relationships at the time points 1, 2 and 3 are also shown. Expanded traces around the reversal potentials. (**d,e**) Transient activation of hyperoxia-evoked whole cell currents by 2 mM Ca^{2+} in HEK293T cells transfected with TRPA1. Representative time courses of outward and inward currents under ramp clamp in hyperoxic solution. Corresponding *I-V* relationships at the time points 1, 2 and 3.

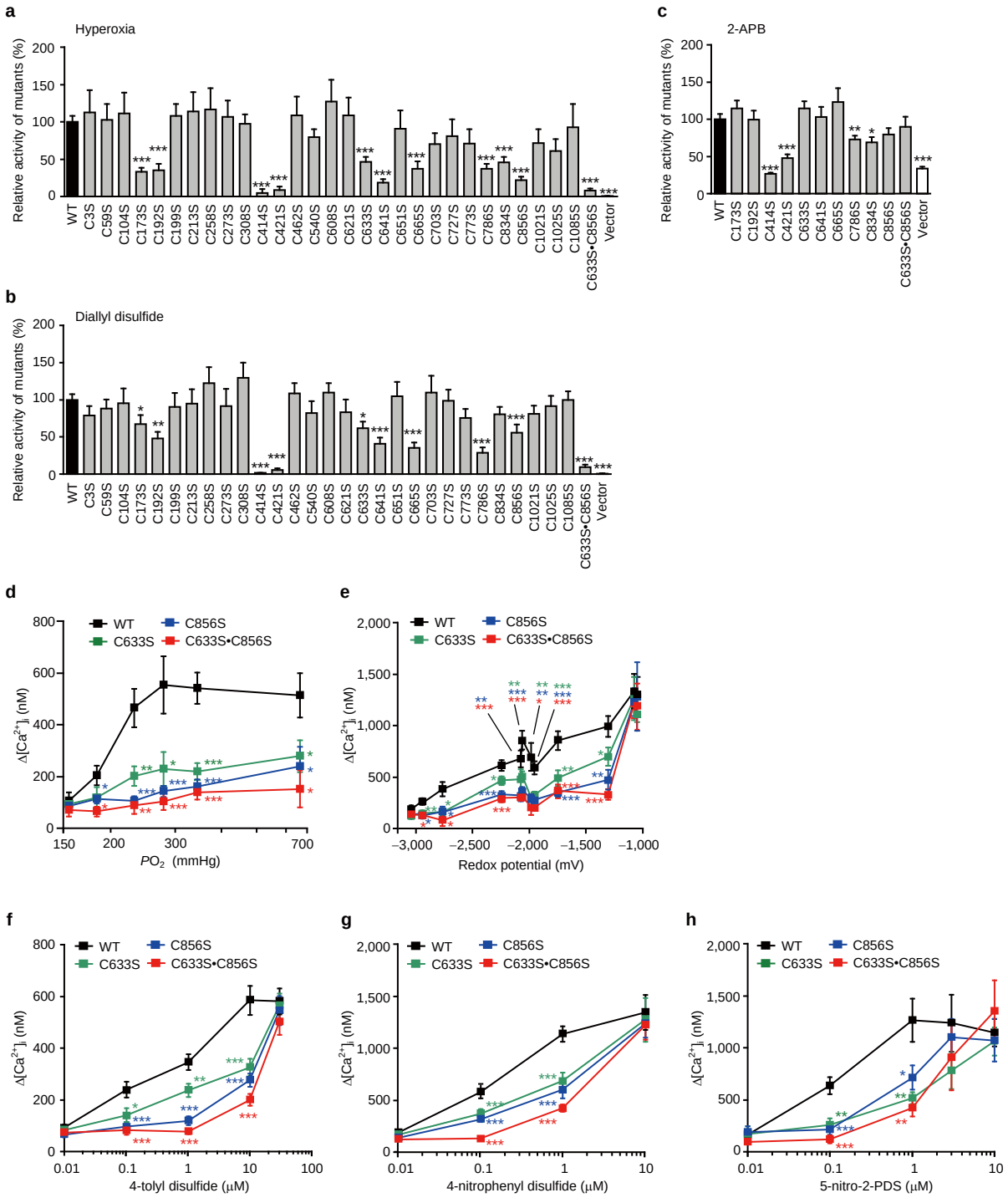

Supplementary Figure 5. Effects of Cys mutations on TRPA1 activation. (**a**,**b**) Relative Ca^{2+} responses of each of TRPA1 Cys mutants to hyperoxia (**a**) (n = 17–109) and 10 μM diallyl disulfide (**b**) (n = 16–44), which has a redox potential comparable to O_2, in HEK293 cells. (**c**) Relative Ca^{2+} responses to 100 μM 2-APB of TRPA1 Cys mutants, which showed impaired response to hyperoxia, in HEK293 cells (n = 20–67). (**d**) The relationships between PO_2 and $\Delta[Ca^{2+}]_i$ mediated by WT TRPA1, C633S, C856S or C633S·C856S in HEK293 cells (n = 17–43). (**e**) Plots of $\Delta[Ca^{2+}]_i$ induced by 10 μM reactive disulfides (see **Figure 1a**) and hyperoxia in HEK293 cells transfected with TRPA1 constructs against redox potentials of respective substances (n = 15–42). The order of redox potential of these compounds is dipropyl disulfide < diallyl disulfide < O_2 < 4-aminophenyl disulfide < 4-methoxyphenyl disulfide < 2-pyridyl disulfide < phenyl disulfide < 4-tolyl disulfide < 4-chlorophenyl disulfide < 3-nitrophenyl disulfide < 4-nitrophenyl disulfide < 5-nitro-2-PDS. (**f**–**h**) Dose-response relationships of 4-tolyl disulfide- (**f**) (n = 17–42), 4-nitrophenyl disulfide- (**g**) (n = 21–42) and 5-nitro-2-PDS-induced $\Delta[Ca^{2+}]_i$ (**h**) (n = 23–45) in HEK293 cells transfected with TRPA1 constructs . $^{*}P < 0.05$, $^{**}P < 0.01$ and $^{***}P < 0.001$ compared to WT. Data points are mean ± s.e.m..

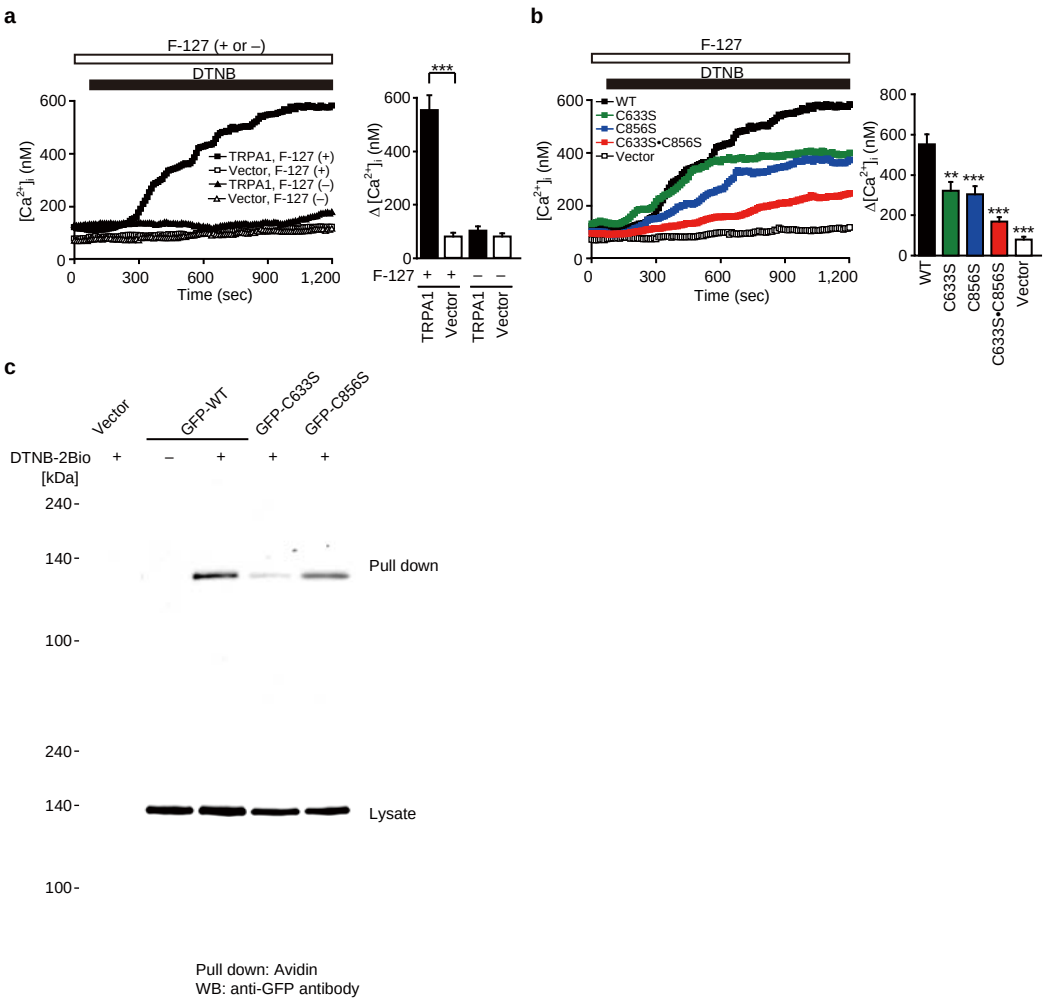

Supplementary Figure 6. DTNB activates TRPA1 only in the presence of F-127. (**a**) TRPA1 responses evoked by 10 μM DTNB in the presence or absence of 0.04% F-127 in HEK293 cells. Ten-min prior to DTNB treatment and continuing during the treatment, cells are incubated with or without F-127. Averaged time courses of $[Ca^{2+}]_i$ changes and $\Delta[Ca^{2+}]_i$ (n = 15–24). DTNB-2Bio fails to activate TRPA1 even in the presence of F-127 (data not shown). Redox potentials ($E_{1/2}$ values) of DTNB and DTNB-2Bio are –1,327 mV and –1,172 mV, respectively. $^{***}P < 0.001$. (**b**) C633S, C856S and C633S·C856S show significantly suppressed responses to DTNB in the presence of F-127. Averaged time courses of $[Ca^{2+}]_i$ changes and $\Delta[Ca^{2+}]_i$ in HEK293 cells transfected by TRPA1 (n = 17–37). $^{**}P < 0.01$ and $^{***}P < 0.001$ compared to WT. (**c**) Full gels and blots of **Figure 2i**. Data points are mean ± s.e.m..

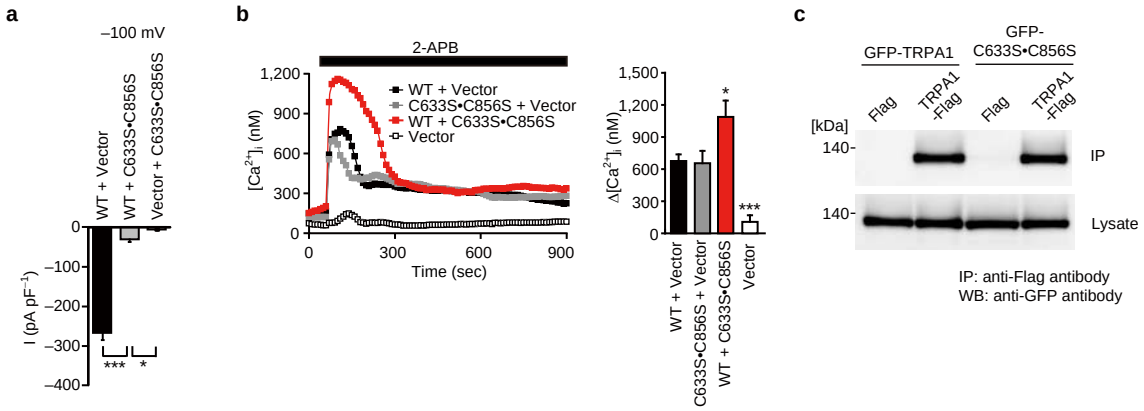

Supplementary Figure 7. Requirement of cysteine oxidation of all four subunits of a TRPA1 channel complex for activation. (a) Hyperoxia-evoked current responses in HEK293T cells transfected with WT TRPA1 (1 μg) and vector (1 μg), WT TRPA1 (1 μg) and C633S·C856S (1 μg) or vector (1 μg) and C633S·C856S (1 μg). Peak current densities at –100 mV in hyperoxic conditions (n = 5–9). $^{*}P <$ 0.05 and $^{***}P < 0.001$. **(b)** Ca^{2+} responses evoked by 100 μM 2-APB in HEK293T cells transfected with WT TRPA1 (1 μg) and vector (1 μg), C633S·C856S (1 μg) and vector (1 μg), WT TRPA1 (1 μg) and C633S·C856S (1 μg) or vector (2 μg). Averaged time courses and $\Delta[Ca^{2+}]_i$ (n = 24–42). $^{*}P < 0.05$ and $^{***}P < 0.001$ compared to HEK293T cells transfected with WT TRPA1 and vector. Data points are mean ± s.e.m.. **(c)** Coimmunoprecipitation of GFP-TRPA1 and GFP-C633S·C856S with TRPA1-Flag. Immunoprecipitates (IP) with antibody to Flag are subjected to WB with antibody to GFP.

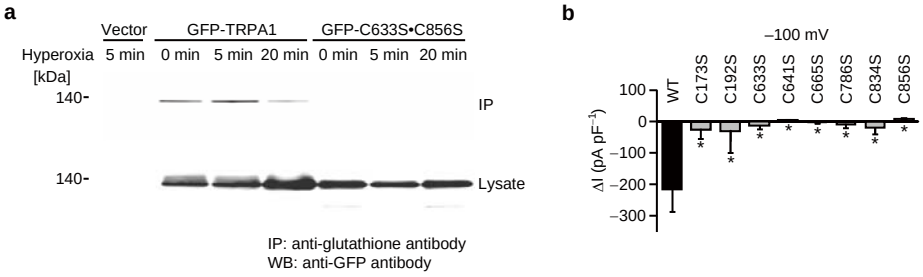

Supplementary Figure 8. Effects of glutathione on TRPA1 Cys mutants. (**a**) Short-term exposure of hyperoxic solution leads to S-glutathionylation of TRPA1. Detection of S-glutathionylation in GFP-TRPA1 or GFP-C633S·C856S channel protein. IP with antibody to glutathione are subjected to WB with antibody to GFP. (**b**) Hyperoxia-evoked current responses (Δ*I*) of TRPA1 Cys mutants in HEK293T cells. Two mM reduced glutathione are internally perfused from the patch pipette. The basal density of whole cell inward currents in normoxia is subtracted from that recorded after treatment with hyperoxic solution at –100 mV (n = 5–7). $^{*}P < 0.05$ compared to WT. Data points are mean ± s.e.m..

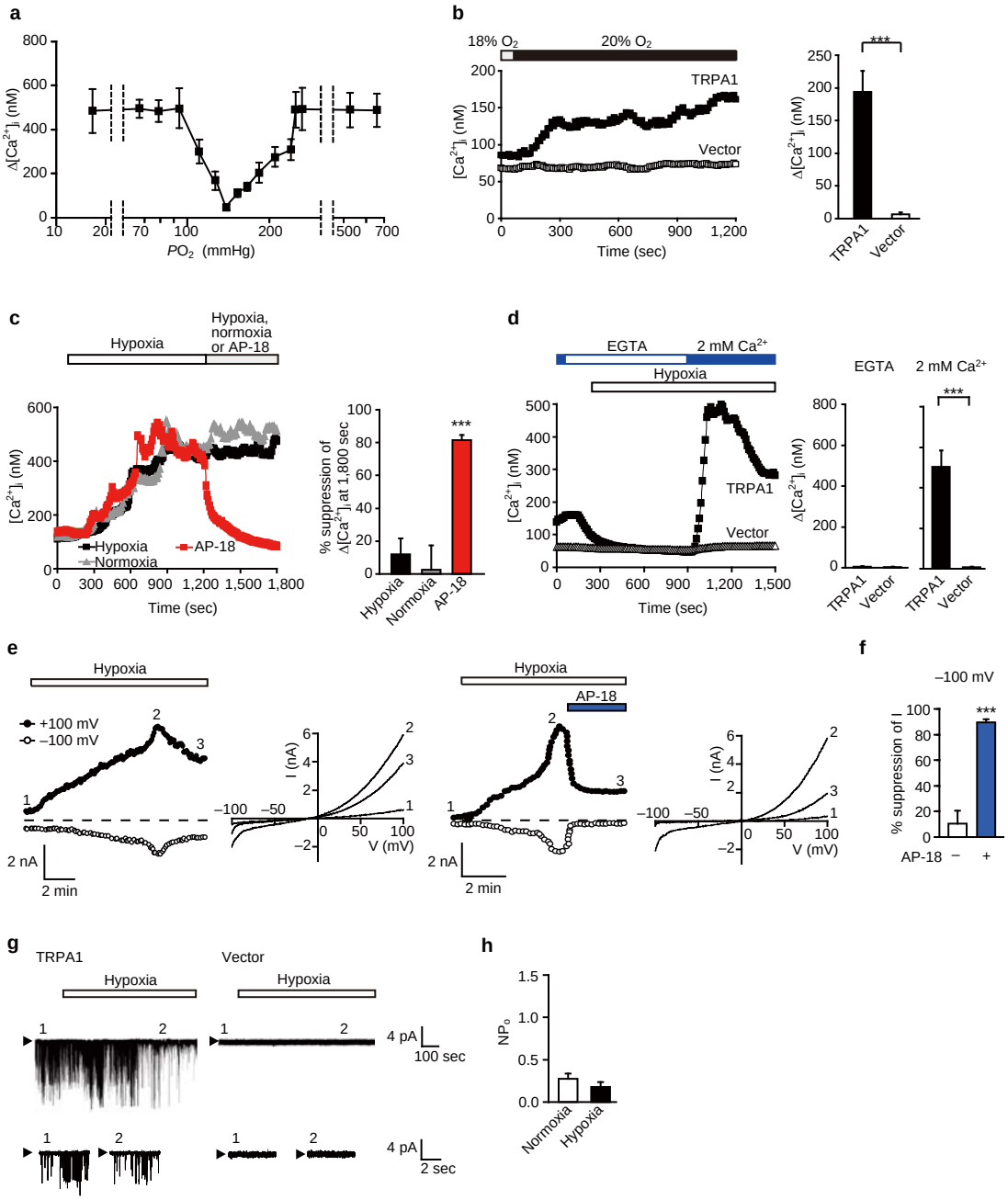

Supplementary Figure 9. TRPA1 channels are activated by hypoxia in the intact cellular configuration but not in cell-excised membrane patches. (a) TRPA1 responses evoked by hyperoxia and hypoxia in bicarbonate/CO_2 buffered solution in HEK293 cells. The relationship between PO_2 and $\Delta[Ca^{2+}]_i$ in TRPA1-expressing HEK293 cells (n = 21–37). (**b**) TRPA1 is activated by changes in PO_2 from 18% (137 mmHg) to 20% (152 mmHg). Averaged time courses and $\Delta[Ca^{2+}]_i$ in TRPA1-expressing HEK293 cells (n = 21–32). $^{***}P < 0.001$. (**c**) Suppression of hypoxia-induced Ca^{2+} responses via TRPA1 by 10 μM AP-18. Averaged time courses and percentage suppression of $[Ca^{2+}]_i$ rises at 1,800 sec relative to $\Delta[Ca^{2+}]_i$ up to 1,200 sec in TRPA1-expressing HEK293 cells (n = 18–26). $^{***}P < 0.001$ compared to cells treated with normoxic solution. (**d**) Averaged time courses and $\Delta[Ca^{2+}]_i$ induced by hypoxia (n = 11–28) in Ca^{2+}-free, 0.5 mM EGTA- or 2 mM Ca^{2+}-containing solution for HEK293 cells transfected with TRPA1 or vector. $^{***}P < 0.001$. (**e**) Suppression of hypoxia-evoked whole cell currents by 10 μM AP-18 in TRPA1-expressing HEK293T cells. Representative time courses of outward and inward currents under ramp clamp. Corresponding I-V relationships at the time points 1–3. (**f**) Suppression of hypoxia-activated TRPA1 currents by AP-18 at –100 mV (n = 10). Percentage suppression of the suppressed current (2–3) at 3-min after the peak relative to the induced current at the peak (2–1). $^{***}P < 0.001$ compared to cells maintained in hypoxia without AP-18. (**g**) Single channel activities in the hypoxic solution at –60 mV in inside-out patches excised from HEK293T cells transfected with TRPA1 or vector. Time-expanded current traces before (trace 1) and during (trace 2) application are also shown in the bottom panels. Arrowheads represent the closed state. (**h**) Averages of NP_O representing single TRPA1 channel activity in normoxia (n = 35) and hypoxia (n = 14). Data points are mean ± s.e.m..

Nature Chemical Biology: doi:10.1038/nchembio.640

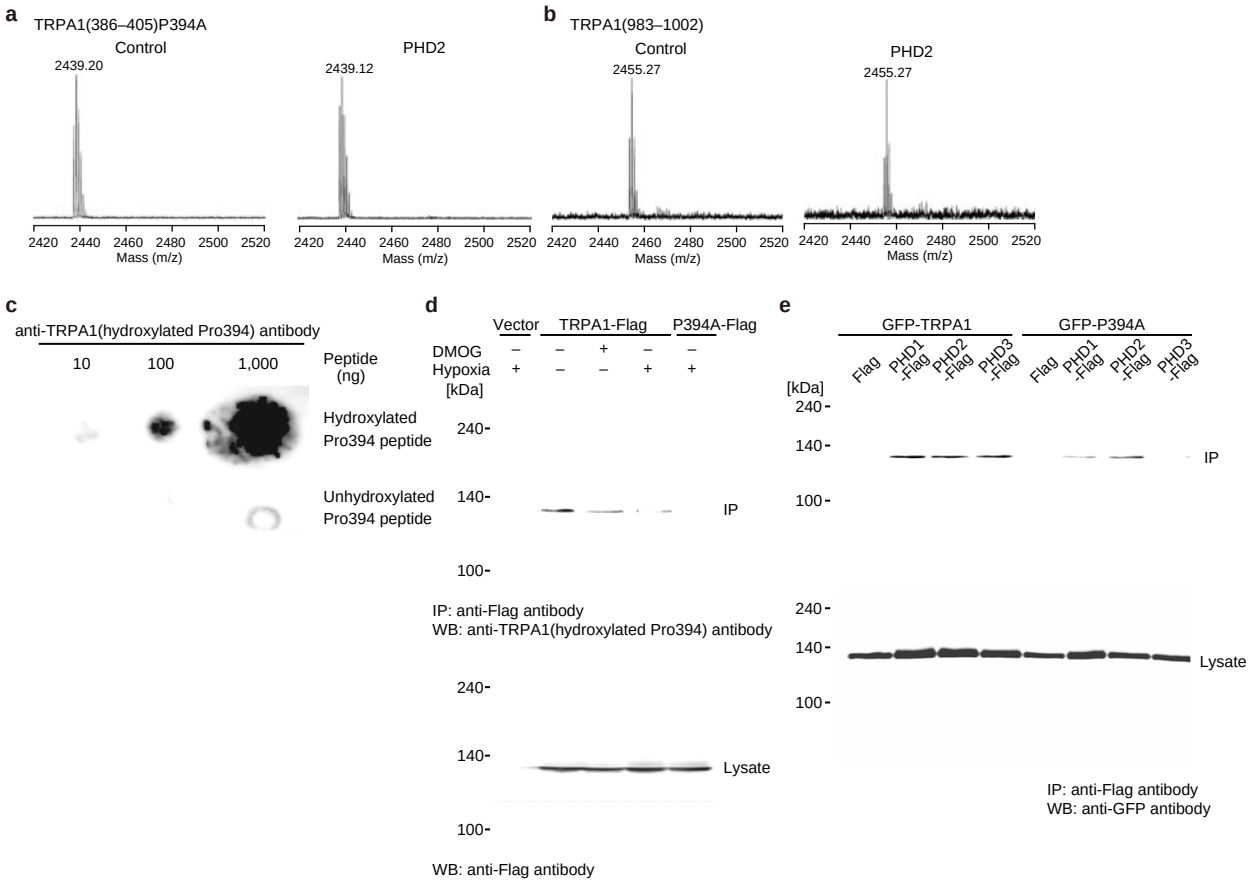

Supplementary Figure 10. Pro394 in TRPA1 is susceptible to hydroxylation by PHDs. (**a,b**) Mass spectrometry analysis of TRPA1 peptides incubated with purified recombinant PHD2. Spectra of the mutant TRPA1(386–405)P394A (**a**) and TRPA1(983–1002) peptides (**b**) are unaffected by PHD2. The peptide sequences of TRPA1(386–405)P394A and TRPA1(983–1002) are PYGLKNLRAEFMQMQQIKEL and HTSLEKKLPLWFLRKVDQKS, respectively. (**c**) TRPA1 (hydroxylated Pro394)-specific antibody selectively recognizes hydroxylated Pro394 of TRPA1 protein. The polyvinylidene fluoride membrane is dotted with 10 ng, 100 ng and 1,000 ng of hydroxylated Pro394 peptide (LKNLRP(OH)EFMQ) (top) and with 10 ng, 100 ng and 1,000 ng of unhydroxylated Pro394 peptide (LKNLRPEFMQ) (bottom). The membrane is subjected to dot-blot with antibody to TRPA1 (hydroxylated Pro394). (**d,e**) Full gels and blots of **Figure 4c,d**.

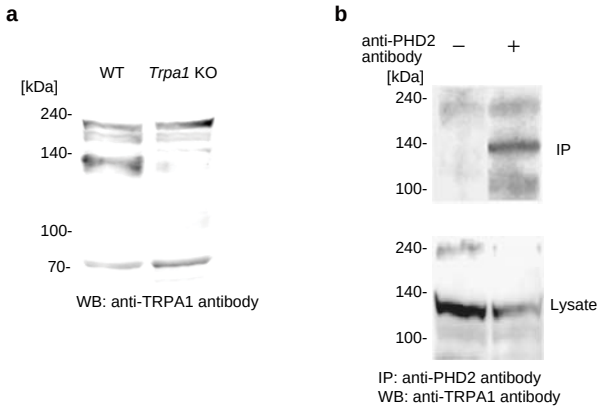

Supplementary Figure 11. Interaction between native PHD2 and TRPA1 protein. (**a**) Protein expression of TRPA1 (calculated molecular weight, 128.5 kDa) is disrupted in DRG from *Trpa1* KO mice. WB is performed using anti-TRPA1 antibody. (**b**) Long exposure for full gels and blots of **Figure 4e**.

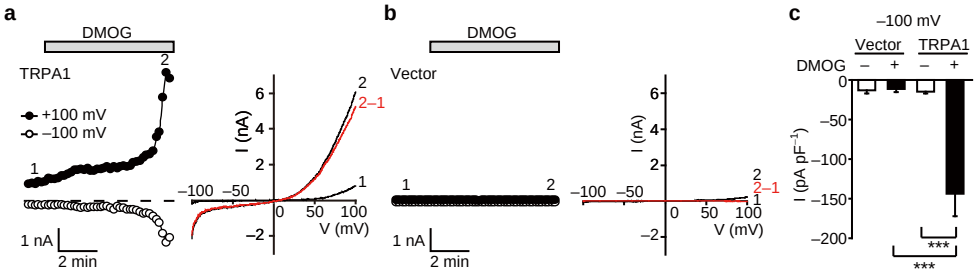

Supplementary Figure 12. DMOG activates TRPA1 channel. (**a,b**) Representative time courses of 300 μM DMOG-evoked outward and inward currents under ramp clamp in HEK293T cells transfected with TRPA1 (**a**) or vector (**b**). Corresponding *I-V* relationships at the time points 1 and 2, and those of evoked currents (2–1) are also shown. (**c**) Peak current densities at –100 mV during the treatment with DMOG or its vehicle (0.01% DMSO) (n = 7–21). $^{***}P < 0.001$. Data points are mean ± s.e.m..

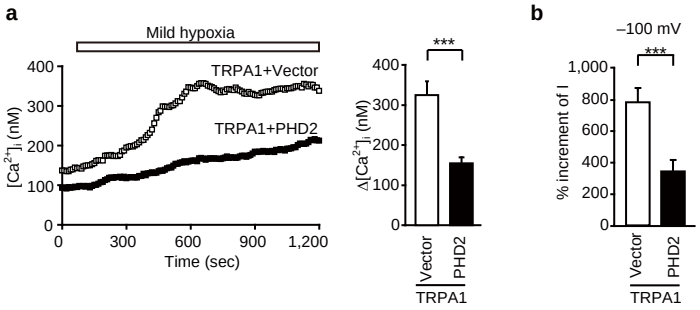

Supplementary Figure 13. Overexpression of PHD2 suppresses the response of TRPA1 to mild hypoxia. (**a**) Ca^{2+} responses to mild hypoxia in TRPA1-expressing HEK293 cells cotransfected with vector or PHD2. Averaged time courses and $\Delta[Ca^{2+}]_i$ (n = 32–42). Dissolved PO_2 measured in mild hypoxic solution is 111 mmHg (14% O_2). $^{***}P < 0.001$. (**b**) Percentage increment of whole cell currents in mild hypoxia at –100 mV in TRPA1-expressing HEK293 cells cotransfected with vector or PHD2 (n = 5–24). $^{***}P < 0.001$. Data points are mean ± s.e.m..

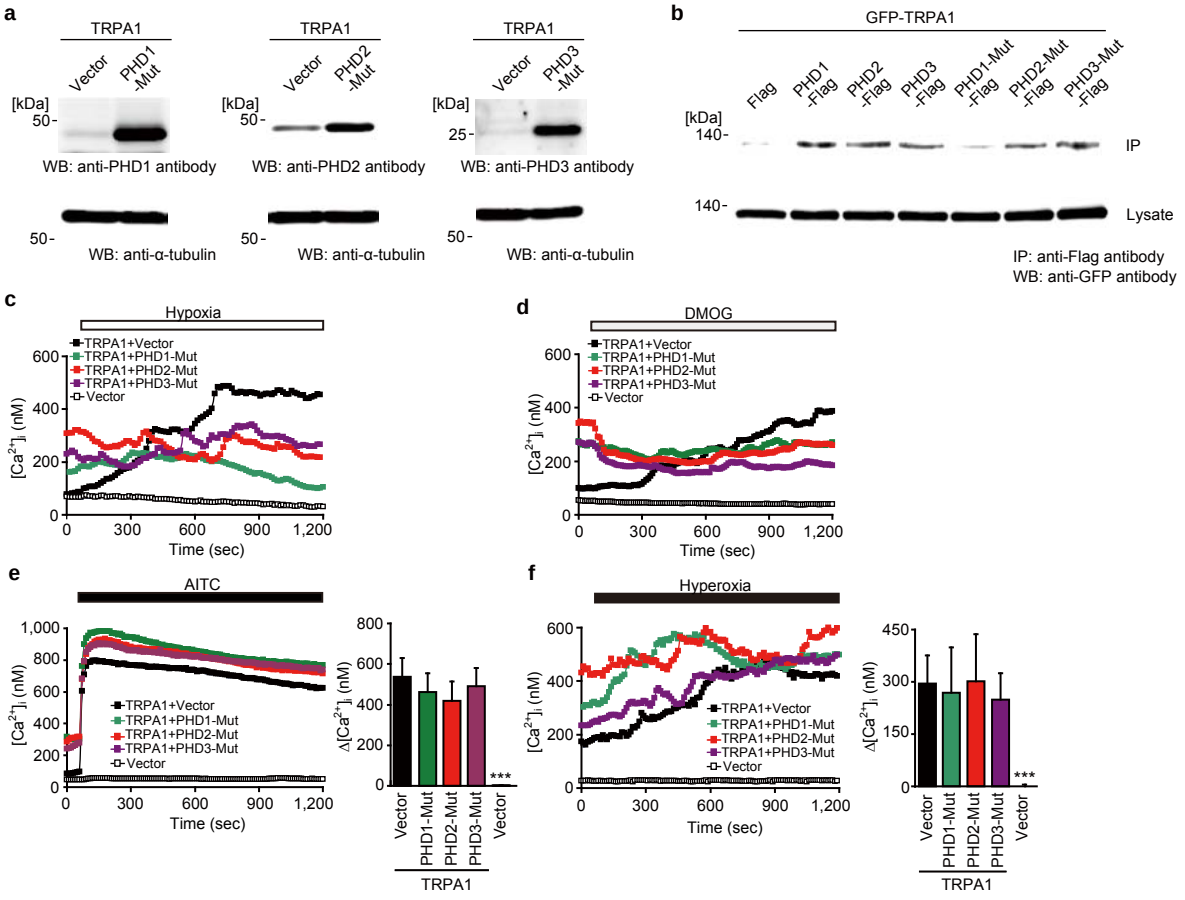

Supplementary Figure 14. TRPA1 responses to hypoxia and DMOG are suppresssed by overexpression of PHD mutants. (**a**) Overexpression of exogenous catalytically dead mutants for PHD1–3 (PHD1-Mut, PHD2-Mut or PHD3-Mut) compared to endogenous PHD1–3 in TRPA1-expressing HEK293 cells cotransfected with vector or PHD1–3 Mut. WB with antibody to PHD1, PHD2 or PHD3 (Novus Biologicals). An anti-α-tubulin antibody (SIGMA) is used as a loading control. (**b**) Coimmunoprecipitation of GFP-TRPA1 with PHD1–3 and PHD1–3 Mut. IP with antibody to Flag are subjected to WB with antibody to GFP. (**c,d**) TRPA1 responses to hypoxia (**c**) and 300 μM DMOG (**d**) are suppressed by overexpression of PHD mutants. Averaged time courses in TRPA1-expressing HEK293 cells cotransfected with PHD mutants (n = 13–50). Basal $[Ca^{2+}]_i$ levels and average $[Ca^{2+}]_i$ rises are shown in **Figure 5e,f**. (**e,f**) AITC and hyperoxia activate TRPA1 in TRPA1-expressing HEK293 cells cotransfected with PHD1-Mut, PHD2-Mut and PHD3-Mut. TRPA1 responses evoked by 100 μM AITC (**e**) (n = 15–25) and hyperoxia (**f**) (n = 16–29) . Averaged time courses and average $[Ca^{2+}]_i$ rises at 1,080–1,200 sec. $^{***}P < 0.001$ compared to cotransfection of TRPA1 with vector. Data points are mean ± s.e.m..

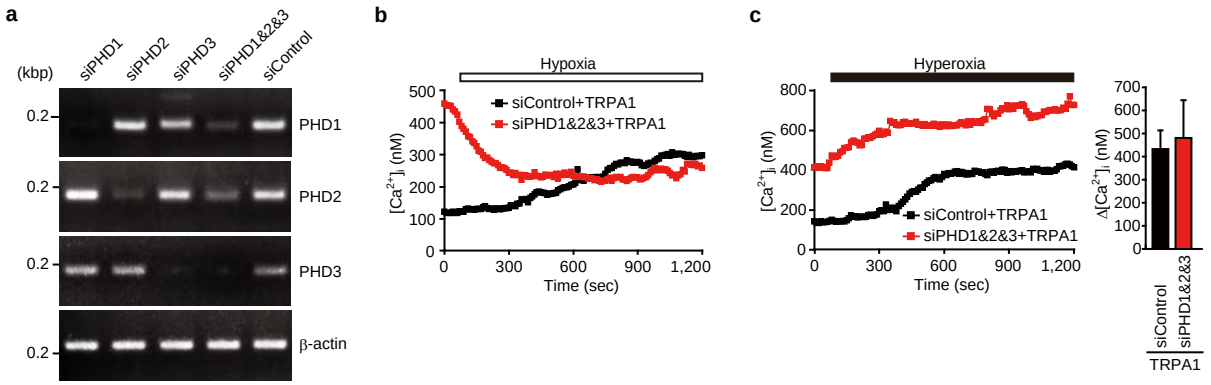

Supplementary Figure 15. TRPA1 responses evoked by hypoxia are suppressed by PHD-specific siRNAs in HEK293 cells. (**a**) RT-PCR analysis of PHD1, PHD2 and PHD3 RNA expression in HEK293 cells treated with PHD1-specific siRNA (siPHD1), PHD2-specific siRNA (siPHD2), PHD3-specific siRNA (siPHD3), a combination of PHD1-, PHD2- and PHD3-specific siRNAs (siPHD1&2&3) and GAPDH siRNA (siControl). β-actin is used as an internal control. (**b**) TRPA1 responses evoked by hypoxia in HEK293 cells treated with siControl or siPHD1&2&3. Averaged time courses (n = 80–147). Basal $[Ca^{2+}]_i$ levels and average $[Ca^{2+}]_i$ rises are shown in **Figure 5g**. (**c**) TRPA1 responses evoked by hyperoxia in HEK293 cells treated with siControl or siPHD1&2&3. Averaged time courses and $\Delta[Ca^{2+}]_i$ (n = 26–40). Data points are mean ± s.e.m..

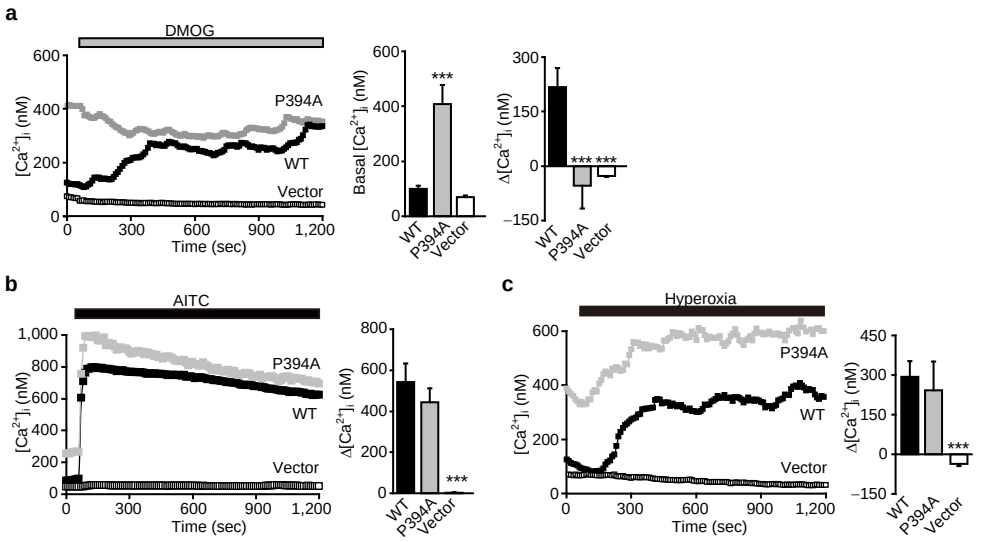

Supplementary Figure 16. P394A mutation greatly enhances spontaneous activation of TRPA1. (**a**) Ca^{2+} responses of TRPA1 constructs to 300 μM DMOG. Averaged time courses, basal $[Ca^{2+}]_i$ levels and average $[Ca^{2+}]_i$ rises at 1,080–1,200 sec in HEK293 cells transfected with TRPA1 costructs (n = 15–21). $^{***}P < 0.001$ compared to WT. (**b,c**) TRPA1 responses evoked by 100 μM AITC (**b**) (n = 18–24) and hyperoxic solution (**c**) are unaffected by P394A mutation (n = 16–20). Averaged time courses and average $[Ca^{2+}]_i$ rises at 1,080–1,200 sec in HEK293 cells transfected with TRPA1 constructs. $^{***}P < 0.001$ compared to WT. Data points are mean ± s.e.m..

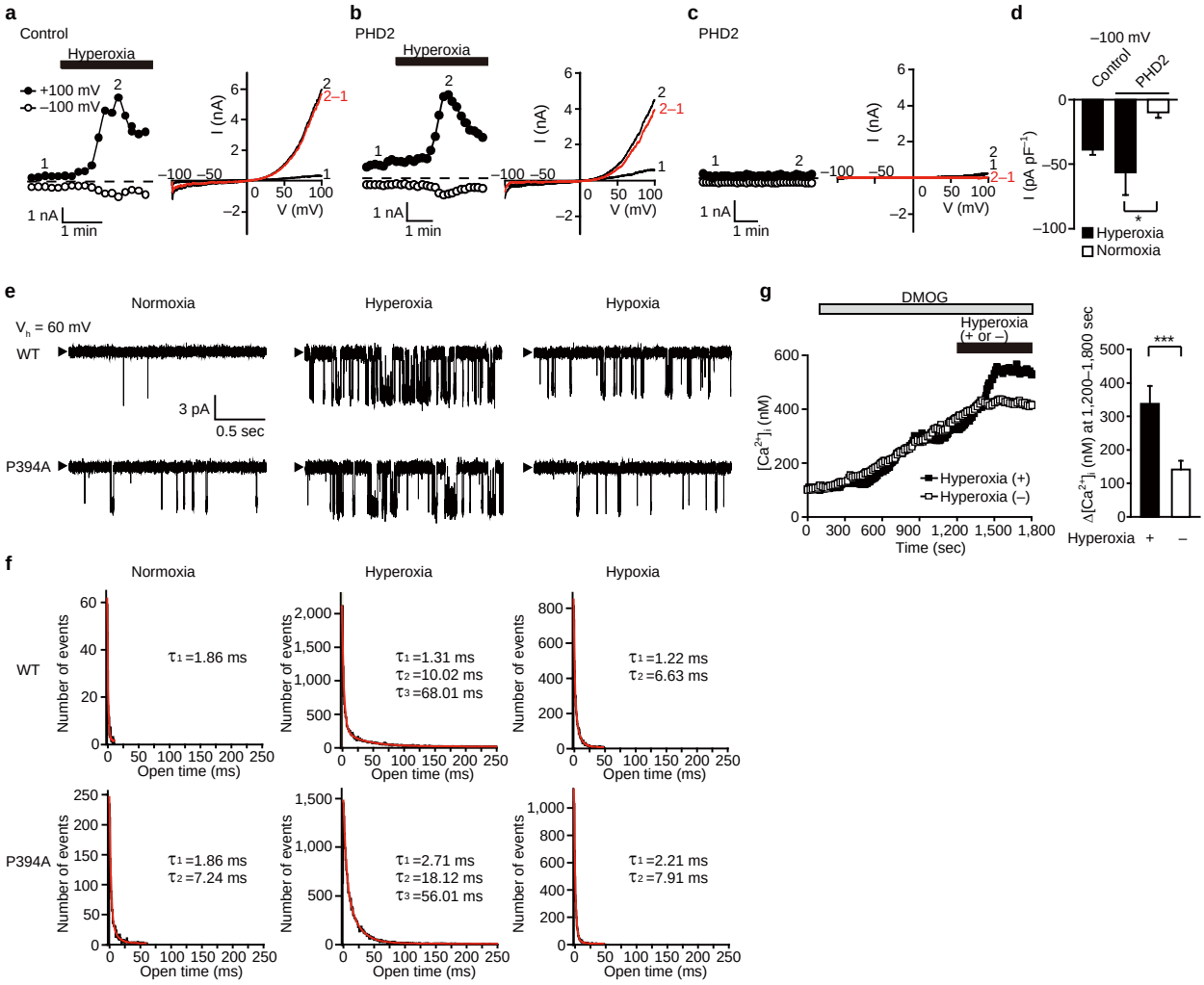

Supplementary Figure 17. O_2 action overrides the PHD-mediated inhibition. (**a–c**) Representative time courses of whole cell currents in hyperoxia (**a,b**) or normoxia (**c**) in TRPA1-expressing HEK293T cells in the absence (**a**) or presence of purified recombinant PHD2 (**b,c**) internally perfused from the patch pipette. Corresponding *I-V* relationships at the time points 1 and 2, and those of evoked currents (2–1) are also shown. (**d**) Peak current densities at –100 mV in the presence or absence of PHD2 in hyperoxia or normoxia (n = 5–8). $^{*}P < 0.05$. (**e,f**) Effects of hyperoxia or hypoxia on channel open state. In (**e**), single channel currents of TRPA1 WT or P394A mutant in normoxia, hyperoxia and hypoxia are recorded at V_h of 60 mV in cell-attached patch are shown. In (**f**), dwell-time histograms of open times in normoxia, hyperoxia and hypoxia are shown. Distributions are best fitted with multiple-exponential functions consisting of one to three exponential components with time constant (τ_1, τ_2 and τ_3). (**g**) Hyperoxia activates TRPA1 even in the presence of DMOG. After incubation with 300 μM DMOG for 19 min, cells are treated with or without hyperoxic solution. Averaged time courses of $[Ca^{2+}]_i$ changes and $\Delta[Ca^{2+}]_i$ at 1,200–1,800 sec in TRPA1-expressing HEK293 cells (n = 22–33). $^{***}P < 0.001$. Data points are mean ± s.e.m.

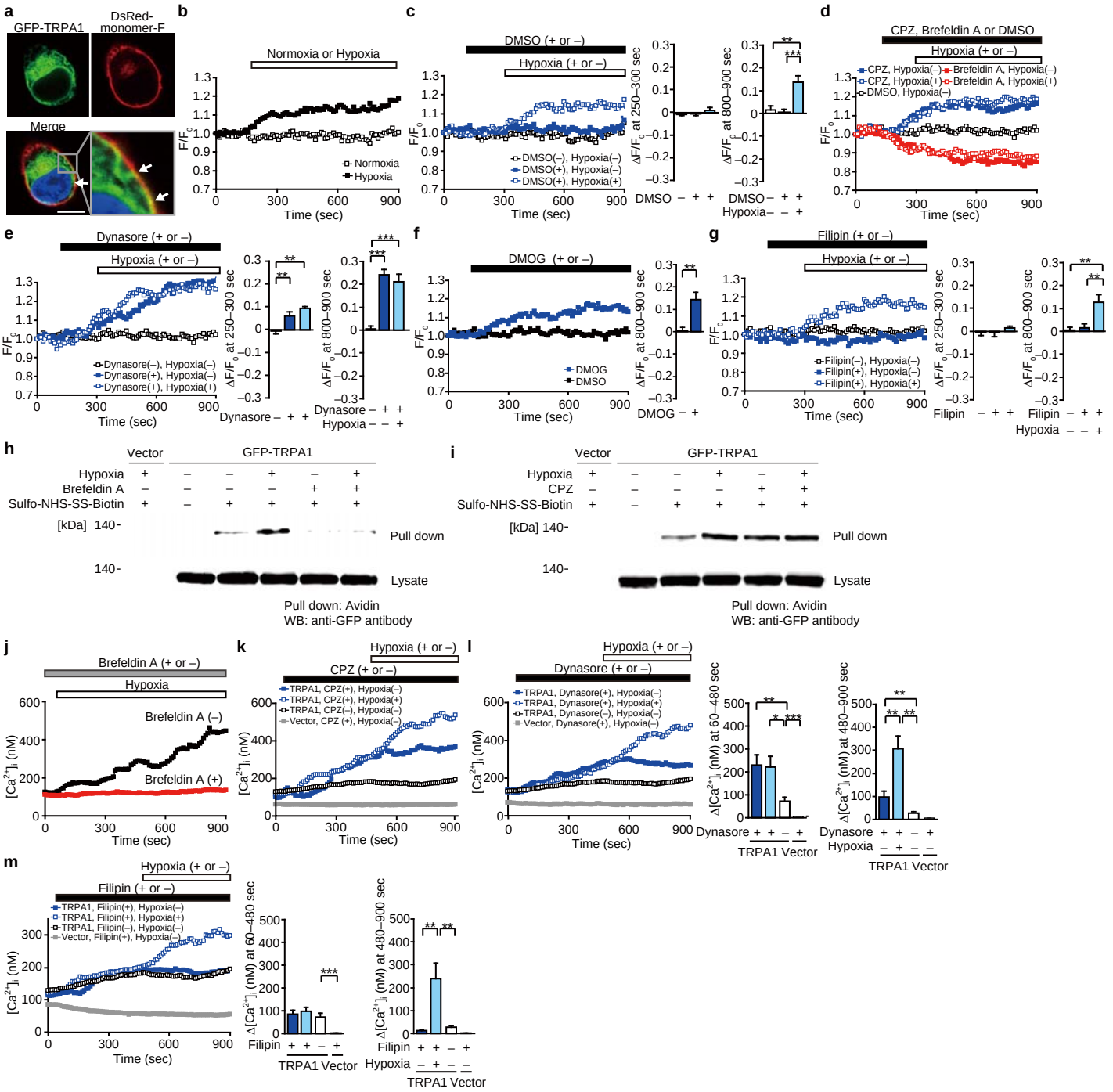

Supplementary Figure 18. Cell surface expression of TRPA1 is enhanced by hypoxia. (**a**) Confocal fluorescent images of HEK293 cells cotransfected with GFP-TRPA1 and the plasmamembrane marker DsRed-monomer-F. Nuclei are stained with Hoechst 33342. Arrows indicate colocalization of TRPA1 with DsRed-monomer-F on the plasmamembrane. The bar indicates 10 μm. (**b**) Cell surface expression of TRPA1 is enhanced by hypoxia. Averaged time courses of surface fluorescence changes (F/F_0) obtained by TIRF images are shown (n = 12–20). Average $\Delta F/F_0$ is shown in **Figure 5j**. (**c–g**) Effects of 0.1% DMSO (**c**), 5 μg ml^{-1} CPZ (**d**), 100 μM brefeldin A (**d**), 80 μM dynasore (**e**), 300 μM DMOG (**f**) and 1 μg ml^{-1} filipin (**g**) on surface fluorescence signal of GFP-TRPA1 in HEK293 cells. In (**c**)–(**e**) and (**g**), after incubation with DMSO (**c**), CPZ (**d**), brefeldin A (**d**), dynasore (**e**) or filipin (**g**) for 3 min, cells are treated with or without hypoxic solution. Averaged time courses of F/F_0 (**c–g**) and average $\Delta F/F_0$ at 250–300 sec (**c,e,g**) and 800–900 sec (**c,e–g**) are shown (n = 12–18). In (**d**), average $\Delta F/F_0$ is shown in **Figure 5k**. $^{**}P < 0.01$ and $^{***}P < 0.001$. (**h,i**) Cell surface expression of GFP-TRPA1. GFP-TRPA1-expressing HEK293 cells are preincubated with 200 μM brefeldin A (**h**) or 5 μg ml^{-1} CPZ (**i**) for 3–4 h, and then incubated with hypoxic solution for 5 min. The cell lysate prepared after exposure to sulfo-NHS-SS-biotin is incubated with streptavidin-agarose, and the obtained proteins are analyzed by WB with anti-GFP antibody. (**j**) Brefeldin A inhibits hypoxia-induced TRPA1 responses. Three hour prior to the treatment with hypoxic solution and continuing during the treatment, cells are incubated with 100 μM brefeldin A. Averaged time courses are shown (n = 27–28). $\Delta[Ca^{2+}]_i$ is shown in **Figure 5l**. (**k–m**) TRPA1 responses evoked by 1 μg ml^{-1} CPZ (**k**), 1 μM dynasore (**l**), 1 μg ml^{-1} filipin (**m**) or their vehicle (0.1% DMSO) (**k–m**) in HEK293 cells. After incubation with CPZ (**k**), dynasore (**l**) or filipin (**m**) for 7 min, cells are treated with or without hypoxic solution. Averaged time courses of $[Ca^{2+}]_i$ changes (**k–m**) and $\Delta[Ca^{2+}]_i$ at 60–480 sec and 480–900 sec (**l,m**) (n = 17–42) are shown. In (**k**), $\Delta[Ca^{2+}]_i$ is shown in **Figure 5m**. $^{*}P < 0.05$, $^{**}P < 0.01$ and $^{***}P < 0.001$. Data points are mean + s.e.m.

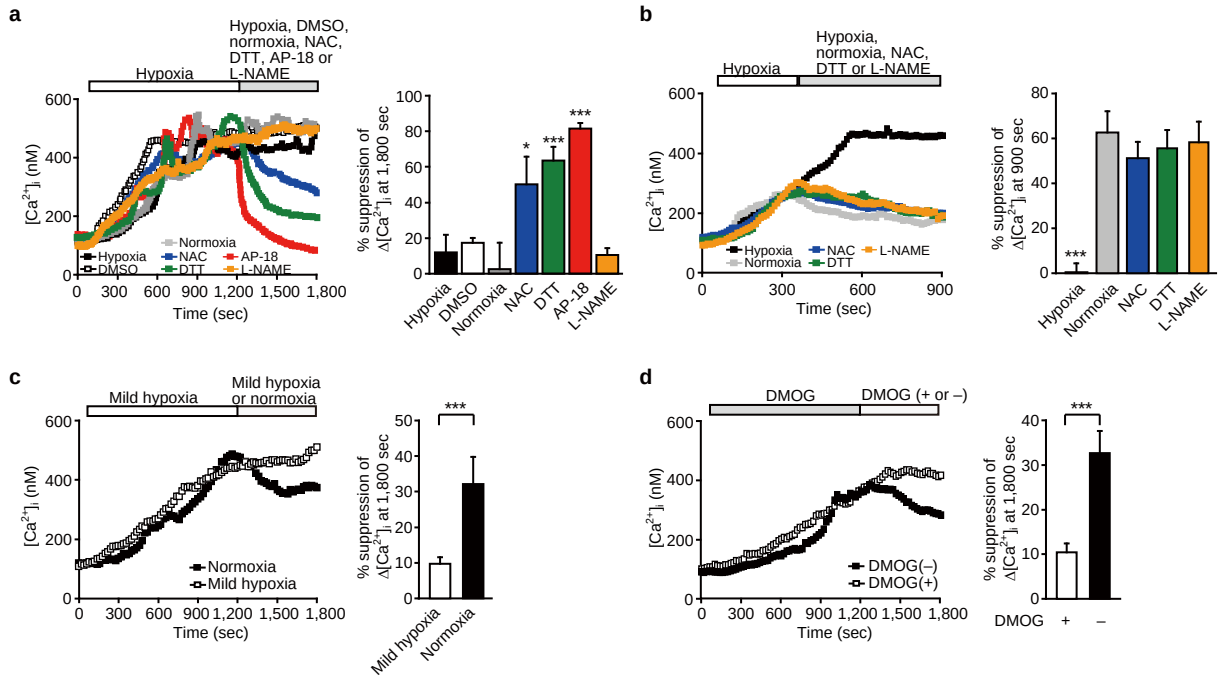

Supplementary Figure 19. Pharmacological characterization of hypoxia-activated TRPA1 responses. (**a**) TRPA1 responses evoked by the 19-min treatment with hypoxic solution are sustained after switching the condition to normoxia alone or in combination with vehicle for AP-18 (0.01% DMSO) or 300 μM L-NAME but are suppressed after switching the condition to normoxia in combination with 1 mM NAC, 1 mM DTT or 10 μM AP-18 in HEK293 cells. Averaged time courses and percentage suppression of $[Ca^{2+}]_i$ rises at 1,800 sec relative to $\Delta[Ca^{2+}]_i$ up to 1,200 sec (n = 12–20). $^{*}P < 0.05$ and $^{***}P < 0.001$ compared to cells treated with normoxic solution. (**b**) TRPA1 responses evoked by the 5-min treatment with hypoxic solution are suppressed after switching the condition to normoxia alone or in combination with 1 mM NAC, 1 mM DTT or 300 μM L-NAME in HEK293 cells. Averaged time courses and percentage suppression of $[Ca^{2+}]_i$ rises at 900 sec relative to $\Delta[Ca^{2+}]_i$ up to 360 sec (n = 25–29). $^{***}P < 0.001$ compared to cells treated with normoxic solution. (**c**) TRPA1 responses evoked by the 19-min treatment with mild hypoxic solution are suppressed by normoxic solution in HEK293 cells. Averaged time courses and percentage suppression of $[Ca^{2+}]_i$ rises at 1,800 sec relative to $\Delta[Ca^{2+}]_i$ up to 1,200 sec (n = 15–27). Dissolved PO_2 measured in mild hypoxic solution is 111 mmHg (14% O_2). $^{***}P < 0.001$. (**d**) TRPA1 responses evoked by the 19-min treatment with 300 μM DMOG are suppressed by wash out (DMOG(–)) in HEK293 cells. Averaged time courses and percentage suppression of $[Ca^{2+}]_i$ rises at 1,800 sec relative to $\Delta[Ca^{2+}]_i$ up to 1,200 sec(n = 19–25). $^{***}P < 0.001$. Data points are mean ± s.e.m..

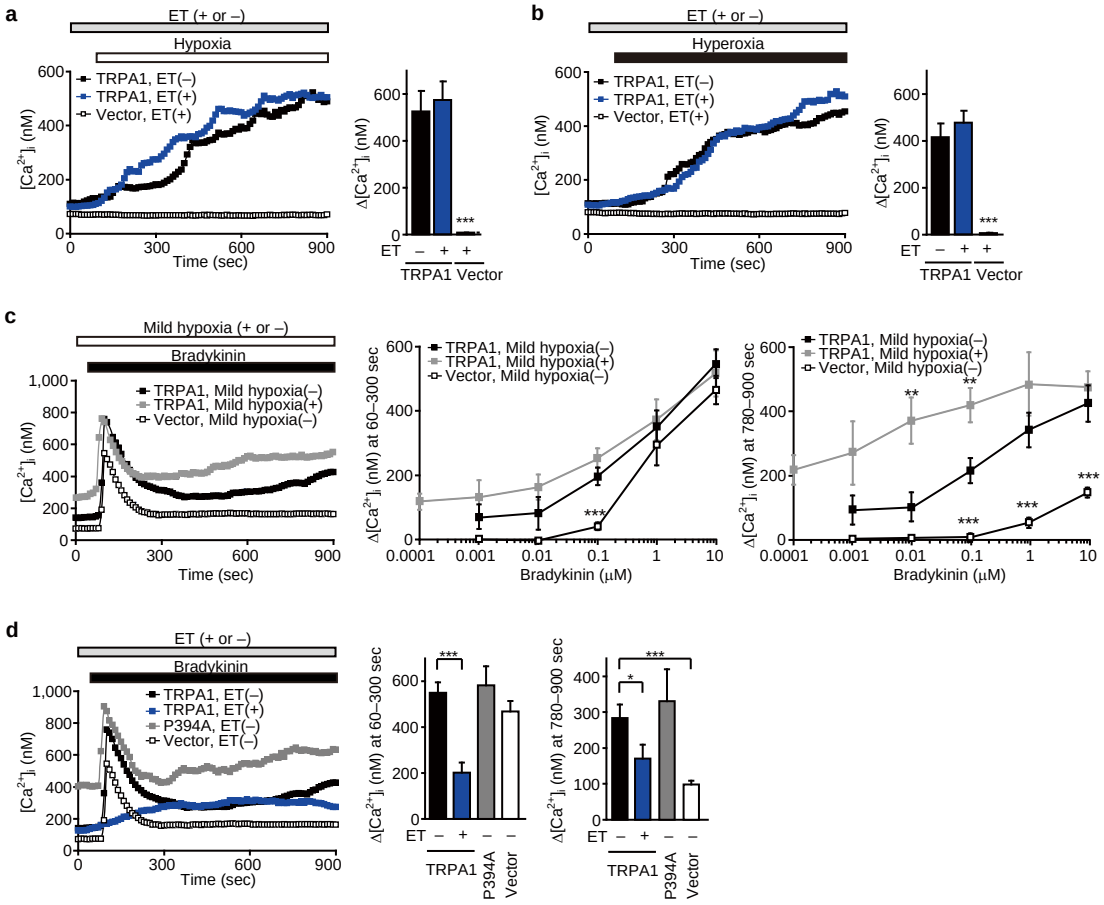

Supplementary Figure 20. Relationship of hydroxylation-dependent regulatory mechanism with PLC-coupled receptor mediated mechanism in TRPA1 activation. (**a,b**) Effect of edelfosine (ET), a PLC inhibitor, on TRPA1 responses evoked by hypoxia (**a**) and hyperoxia (**b**) in HEK293 cells. Five-min prior to the treatment with hypoxic (**a**) or hyperoxic (**b**) solution and continuing during the treatment, cells are incubated with 1 μM ET or its vehicle (0.1% ethanol). Averaged time courses and Δ $[Ca^{2+}]_i$ (n = 16–31). $^{***}P < 0.001$ compared to TRPA1 without ET. (**c**) Effect of mild hypoxia on TRPA1 responses evoked by bradykinin in bradykinin receptor 2 (B_2R)-expressing HEK293 cells. Averaged time courses of $[Ca^{2+}]_i$ changes evoked by 10 μM bradykinin and dose-response relationships of Δ$[Ca^{2+}]_i$ at 60–300 sec or 780–900 sec (n = 19–42). Dissolved PO_2 measured in mild hypoxic solution is 111 mmHg (14% O_2). $^{**}P < 0.01$ and $^{***}P < 0.001$ compared to TRPA1 (mild hypoxia(–)). (**d**) TRPA1 responses to bradykinin are unaffected by P394A mutation. TRPA1 responses evoked by 10 μM bradykinin in the presence or absence of 1 μM ET in B_2R-expressing HEK293 cells transfected with TRPA1 constructs. Five-min prior to bradykinin treatment and continuing during the treatment, cells are incubated with 1 μM ET or its vehicle (0.1% ethanol). Averaged time courses of $[Ca^{2+}]_i$ changes and Δ $[Ca^{2+}]_i$ at 60–300 sec or 780–900 sec (n = 29–39). $^{*}P < 0.05$ and $^{***}P < 0.001$. Data points are mean ± s.e.m..

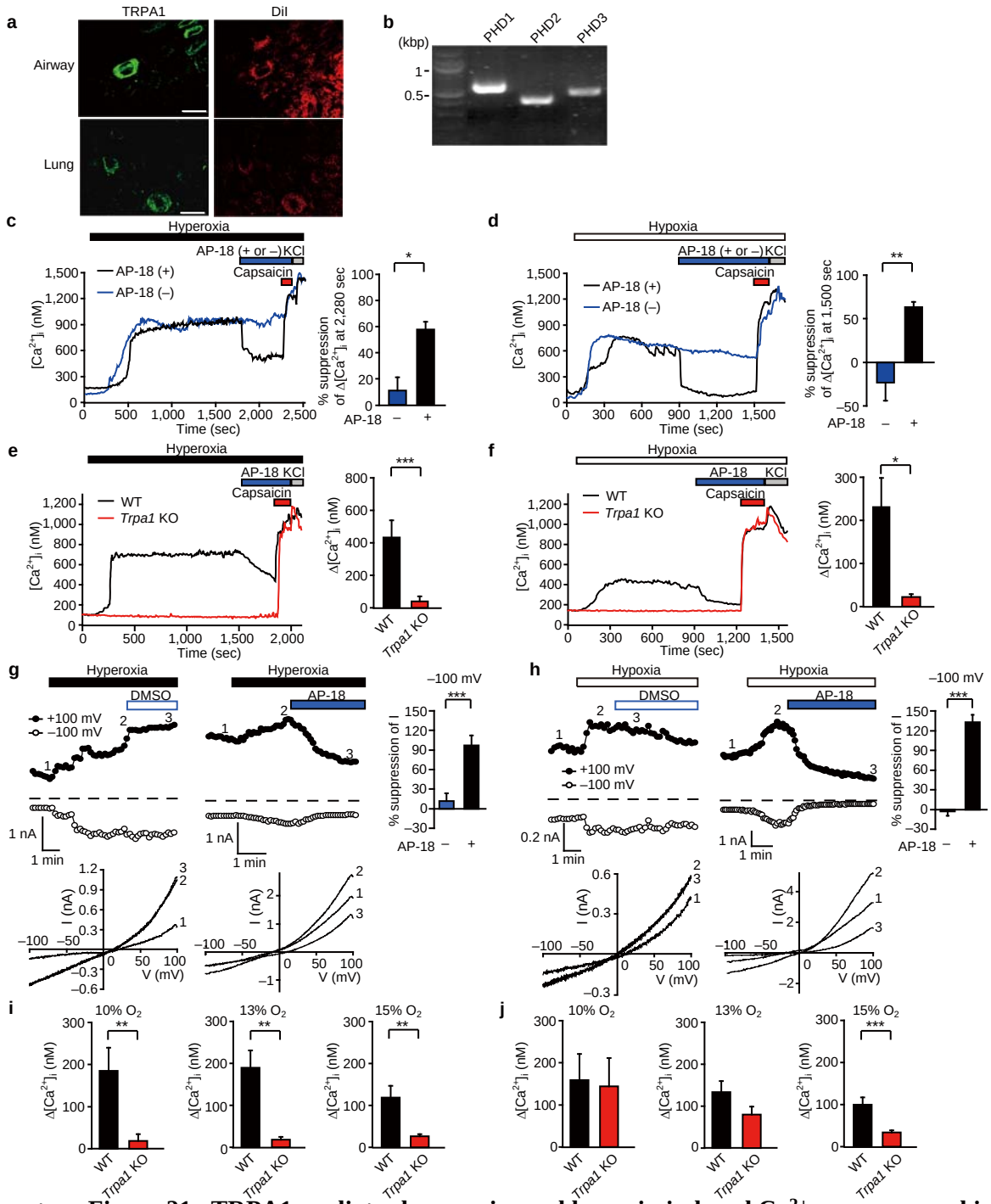

Supplementary Figure 21. TRPA1 mediates hyperoxia- and hypoxia-induced Ca^{2+} responses and ionic currents in mouse nodose ganglion neurons. (**a**) Expression of TRPA1 proteins in a subset of nodose ganglion neurons innervating the airway and the lung. Confocal images of immunostaining with TRPA1-specific antibody (green). Retrograde labeling of nodose ganglion neurons projecting to airway or lung with DiI (red) is attained by its instillation into the airway lumen or by transdermal injection into the lung, respectively. The bar indicates 20 μm. (**b**) RNA expression of PHD1–3 detected by RT-PCR in mouse nodose ganglion neurons. (**c,d**) Suppression of hyperoxia- (**c**) and hypoxia-induced Ca^{2+} responses (**d**) by AP-18 in WT nodose ganglion neurons. Representative Ca^{2+} responses evoked in hyperoxic (**c**) or hypoxic (**d**) solution and by application of 10 μM AP-18, vehicle for AP-18 (0.01% DMSO), 3 μM capsaicin and 60 mM KCl and percentage suppression of $[Ca^{2+}]_i$ rises at 2,280 sec (**c**) and 1,500 sec (**d**) relative to Δ $[Ca^{2+}]_i$ up to 1,800 sec (**c**) and 900 sec (**d**) in hyperoxia- (**c**) and hypoxia-responding neurons (**d**), respectively (n = 6–11). $^{*}P < 0.05$ and $^{**}P < 0.01$. (**e,f**) Hyperoxia- (**e**) and hypoxia-induced Ca^{2+} responses (**f**) are ablated in *Trpa1* KO nodose ganglion neurons. Representative Ca^{2+} responses evoked in bicarbonate/CO_2 buffer bubbled with hyperoxic (**e**) (n = 15–20) or hypoxic gas (**f**) (n = 14–38) and $\Delta[Ca^{2+}]_i$ at 60–1,500 sec (**e**) or 60–900 sec (**f**) in capsaicin-sensitive neurons. $^{*}P < 0.05$ and $^{***}P < 0.001$. (**g,h**) Suppression of hyperoxia- (**g**) (n = 6–7) and hypoxia-evoked whole cell currents (**h**) (n = 5–7) by 10 μM AP-18 in WT nodose ganglion neurons. Representative time courses of outward and inward currents under ramp clamp in hyperoxic (**g**) or hypoxic (**h**) solution. Corresponding *I-V* relationships at the time points 1–3. Percentage suppression of the suppressed current (2–3) at 3-min after the peak relative to the induced current at the peak (2–1). $^{***}P < 0.001$. (**i,j**) $[Ca^{2+}]_i$ rises evoked by hypoxia (10, 13 or 15% O_2) in capsaicin-sensitive (**i**) or all nodose ganglion neurons (**j**) (n = 25–192). Dissolved PO_2 measured in the hypoxic solutions are 79 mmHg (10% O_2), 103 mmHg (13% O_2) and 119 mmHg (15% O_2). $^{**}P < 0.01$ and $^{***}P < 0.001$. Data points are mean ± s.e.m..

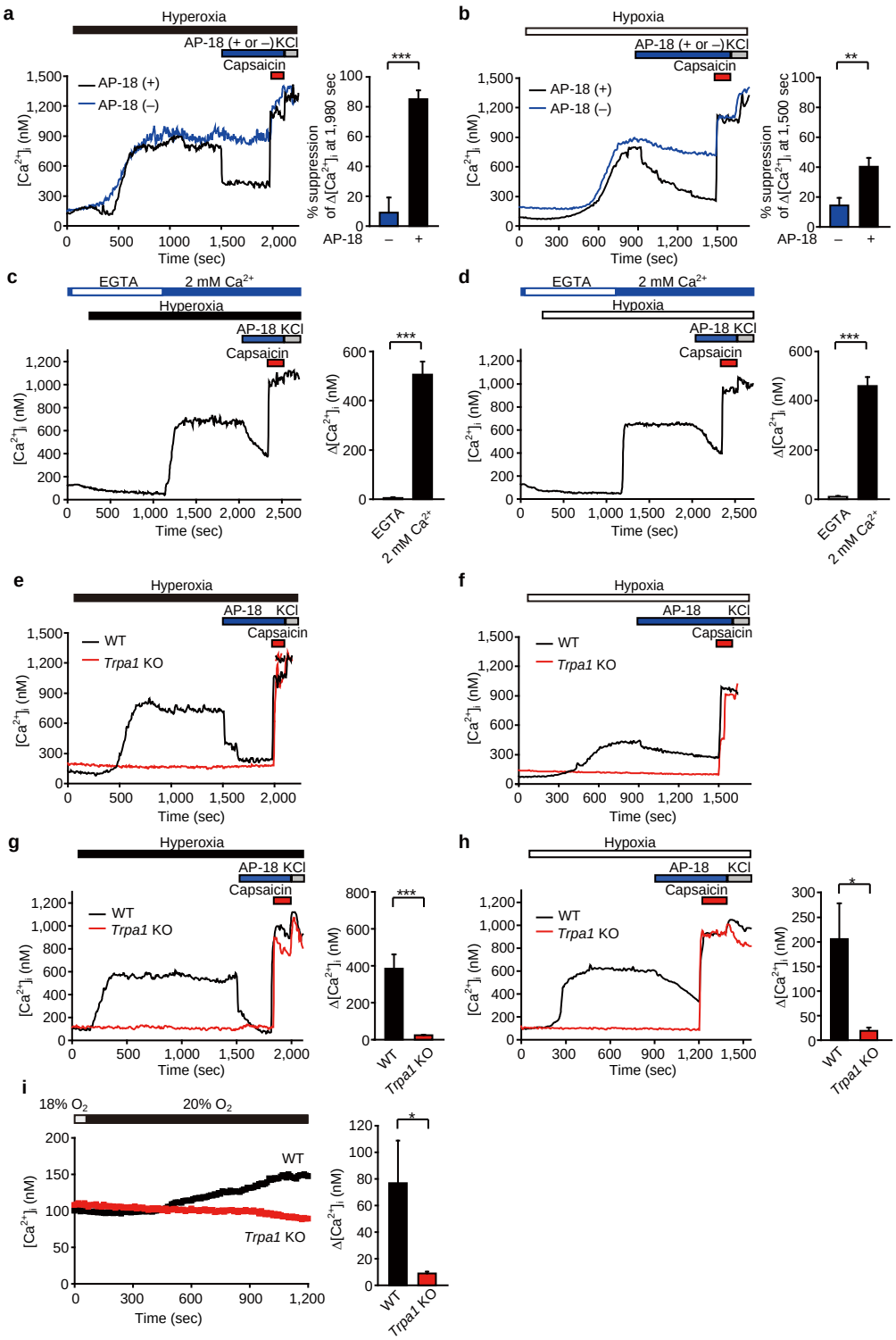

Supplementary Figure 22. Hyperoxia and hypoxia evoke TRPA1 responses in mouse DRG neurons. (**a,b**) Suppression of hyperoxia- (**a**) and hypoxia-induced Ca^{2+} responses (**b**) by AP-18 in WT DRG neurons. Representative Ca^{2+} responses evoked in hyperoxic or hypoxic solution and by application of 10 μM AP-18, vehicle for AP-18 (0.01% DMSO), 3 μM capsaicin and 60 mM KCl and percentage suppression of $[Ca^{2+}]_i$ rises at 1,980 sec (**a**) and 1,500 sec (**b**) relative to $\Delta[Ca^{2+}]_i$ up to 1,500 sec (**a**) and 900 sec (**b**) in neurons responding to hyperoxia (**a**) and hypoxia (**b**), respectively (n = 11–35). $^{**}P < 0.01$ and $^{***}P < 0.001$. (**c,d**) Ca^{2+} influx is responsible for $[Ca^{2+}]_i$ elevation by hyperoxia and hypoxia in mouse DRG neurons. Representative Ca^{2+} response and $\Delta[Ca^{2+}]_i$ induced by hyperoxia (**c**) (n = 31) or hypoxia (**d**) (n = 35) in Ca^{2+}-free, 0.5 mM EGTA- or 2 mM Ca^{2+}-containing solution are shown for capsaicin-sensitive neurons DRG neurons. $^{***}P < 0.001$. (**e,f**) Ablated Ca^{2+} responses to hyperoxia (**e**) and hypoxia (**f**) in capsaicin-sensitive *Trpa1* KO DRG neurons. Representative Ca^{2+} responses are shown. $\Delta[Ca^{2+}]_i$ is shown in **Figure 6i**. (**g,h**) Ablated Ca^{2+} responses to hyperoxia (**g**) and hypoxia (**h**) in capsaicin-sensitive *Trpa1* KO DRG neurons. Representative Ca^{2+} responses evoked in bicarbonate/CO_2 buffer bubbled with hyperoxic (**g**) (n = 23–25) or hypoxic gas (**h**) (n = 13–47) and hyperoxia- (**g**) or hypoxia-induced $\Delta[Ca^{2+}]_i$ (**h**). $^{*}P < 0.05$ and $^{***}P < 0.001$. (**i**) TRPA1 is activated by changes in PO_2 from 18% (137 mmHg) to 20% (152 mmHg). Averaged time courses and $\Delta[Ca^{2+}]_i$ in DRG neurons isolated from WT or *Trpa1* KO mice (n = 46–49). $^{*}P < 0.05$. Data points are mean ± s.e.m..

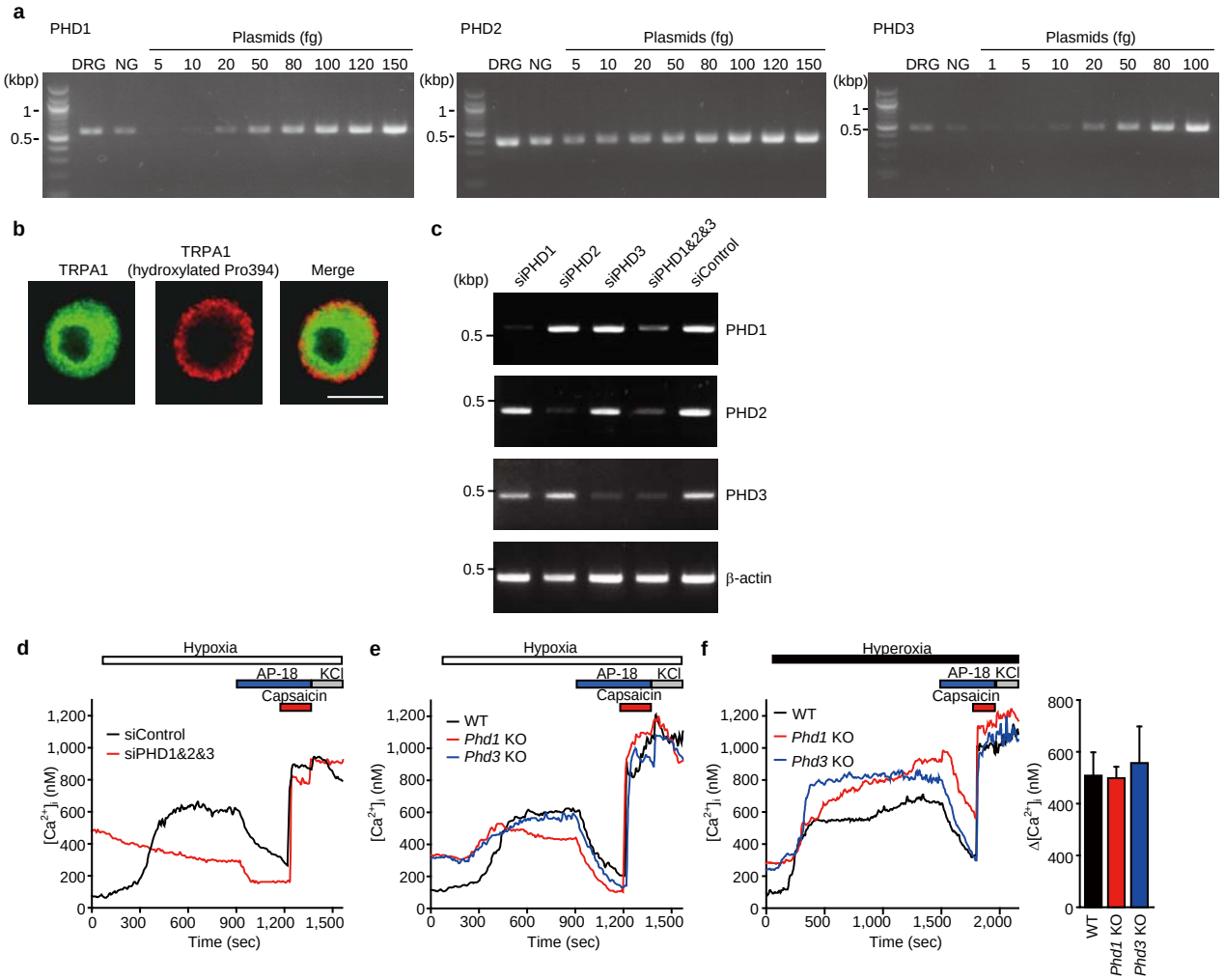

Supplementary Figure 23. PHD-mediated inhibition of TRPA1 channels. (**a**) Semi-quantitative RT-PCR analysis of PHD1, PHD2 and PHD3 RNA expression in mouse DRG and nodose ganglion (NG) neurons. Plasmids carrying PHD1, PHD2 or PHD3 cDNA are used as control. (**b**) Detection of hydroxylated Pro394 of TRPA1 in mouse DRG neurons. Confocal images of immunostaining with TRPA1-specific antibody (green) and TRPA1(hydroxylated Pro394)-specific antibody (red). The bar indicates 10 μm. (**c**) RT-PCR analysis of PHD1, PHD2 and PHD3 RNA expression in mouse DRG neurons treated with PHD1-specific siRNA (siPHD1), PHD2-specific siRNA (siPHD2), PHD3-specific siRNA (siPHD3), a combination of PHD1-, PHD2- and PHD3-specific siRNAs (siPHD1&2&3) and non-targeting siRNA (siControl). β-actin is used as an internal control. (**d**) Ca^{2+} responses to hypoxia in DRG neurons treated with siControl or siPHD1&2&3. Representative Ca^{2+} responses evoked in hypoxic solution and by application of 10 μM AP-18, 3 μM capsaicin and 60 mM KCl in capsaicin-sensitive neurons. Basal $[Ca^{2+}]_i$ levels and average $[Ca^{2+}]_i$ rises are shown in **Figure 6j**. (**e,f**) Ca^{2+} responses to hypoxia (**e**) or hyperoxia (**f**) in *Phd1* or *Phd3* KO DRG neurons. In (**e**), representative Ca^{2+} responses evoked in hypoxic solution are shown. Basal $[Ca^{2+}]_i$ levels and $\Delta[Ca^{2+}]_i$ rises are shown in **Figure 6k**. In (**f**), representative Ca^{2+} responses evoked in hyperoxic solution are shown. $\Delta[Ca^{2+}]_i$ is measured at 60–1,500 sec in capsaicin-sensitive neurons (n = 22–59). Data points are mean ± s.e.m..

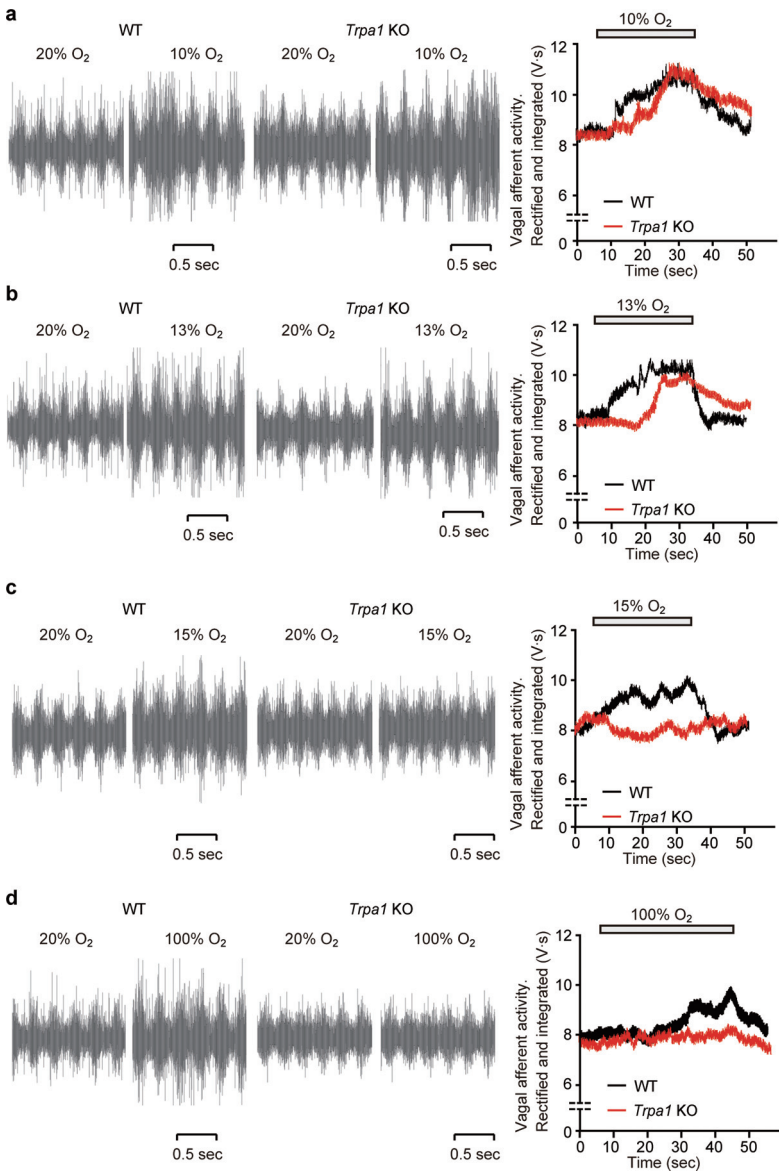

Supplementary Figure 24. Defects of vagal afferent discharges under systemic hypoxia and hyperoxia in *Trpa1* KO mice. Responses of vagal afferent discharges to inhalation of hypoxic gas (10% O_2 for (**a**), 13% O_2 for (**b**) or 15% O_2 for (**c**)) or hyperoxic (100% O_2 for (**d**)) in *Trpa1* KO mice. Representative tracings of vagal afferent discharges. Right panels show rectified and integrated vagal afferent activities. Comparison of percentage changes in rectified and integrated vagal nerve activity in response to inhalation of hypoxic or hyperoxic gas between WT and *Trpa1* KO mice is shown in **Figure 7**.

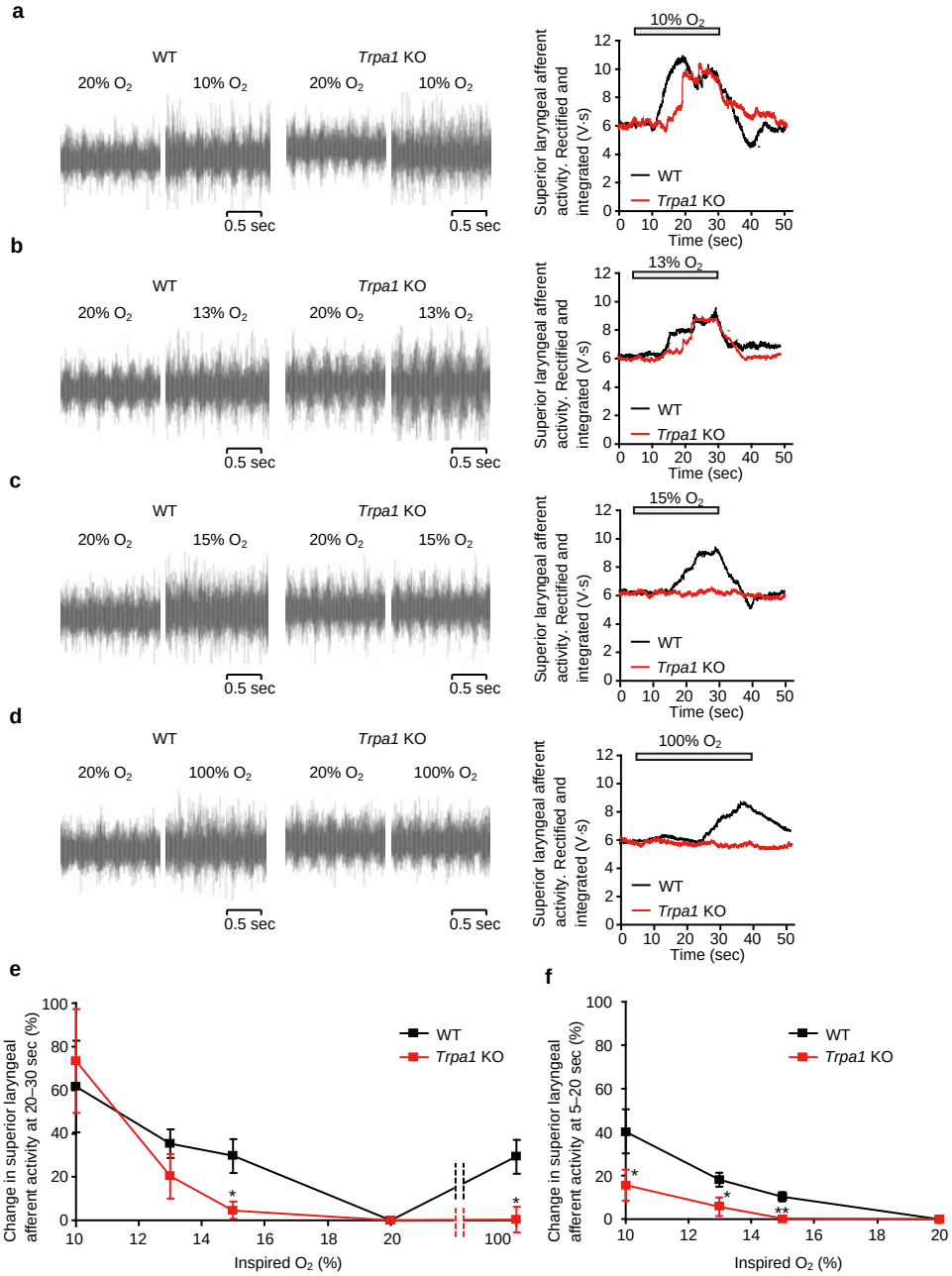

Supplementary Figure 25. Defects of superior laryngeal afferent discharges under systemic hypoxia and hyperoxia in *Trpa1* KO mice. (**a–d**) Responses of superior laryngeal afferent discharges to inhalation of hypoxic gas (10% O_2 for (**a**), 13% O_2 for (**b**) or 15% O_2 for (**c**)) or hyperoxic (100% O_2 for (**d**)) in *Trpa1* KO mice. Representative tracings of superior laryngeal afferent discharges. Right panels show rectified and integrated superior laryngeal afferent activities. (**e,f**) Comparison of percentage changes in rectified and integrated superior laryngeal nerve activity in response to inhalation of hypoxic (10, 13 and 15% O_2) or hyperoxic (100% O_2) gas between WT and *Trpa1* KO mice in the sustained phase (20–30 sec) (**e**) or in the rising phase 5–20 sec (**f**) (n = 4–7). Values denote percentage changes from basal activities recorded during normoxic gas (20% O_2) exposure. $^{*}P < 0.05$ and $^{**}P < 0.01$ compared to WT. Data points are mean ± s.e.m..

Supplementary Table 1. Time constants and relative weights of single channel current measured from cell-attached patches at a holding potential of 60 mV. Open times and their corresponding relative weights for TRPA1 (WT) or P394A mediated currents evoked by hyperoxia and hypoxia. τ_1, τ_2 and τ_3 are time constants and A_1, A_2 and A_3 are relative weights under the respective time constant. $^{*}P < 0.05$, $^{**}P < 0.01$ and $^{***}P < 0.001$ compared to cells maintained in normoxa . Data are mean ± s.e.m..

V_h = 60 mV

WT	Normoxia	Hyperoxia	Hypoxia
Time constants (ms)			
τ_1	1.39 ± 0.15	1.55 ± 0.18	1.47 ± 0.21
τ_2	5.27 ± 0.42	8.88 ± 1.08*	6.85 ± 0.56
τ_3		48.15 ± 14.08	
Relative weights			
A_1	0.95 ± 0.02	0.83 ± 0.02**	0.72 ± 0.04***
A_2	0.05 ± 0.02	0.15 ± 0.02*	0.28 ± 0.04***
A_3		0.02 ± 0.01	

P394A	Normoxia	Hyperoxia	Hypoxia
Time constants (ms)			
τ_1	1.16 ± 0.16	2.76 ± 0.15***	1.51 ± 0.44
τ_2	6.09 ± 0.51	15.84 ± 2.12*	6.38 ± 1.53
τ_3		60.74 ± 13.41	
Relative weights			
A_1	0.73 ± 0.02	0.80 ± 0.04	0.77 ± 0.02
A_2	0.26 ± 0.02	0.14 ± 0.03*	0.22 ± 0.02
A_3		0.05 ± 0.01	

Supplementary Table 2. Hyperoxia and hypoxia responses in nodose ganglion or DRG neurons. The percentages of hyperoxia- and hypoxia-responding neurons are shown. Neurons exposed to hyperoxic or hypoxic solution are treated sequentially with 10 μM AP-18 or 0.01% DMSO, 3 μM capsaicin and 60 mM KCl during periods indicated in **Figure 6a,b** and **Supplementary Figure 21c,d** for nodose ganglion and **Supplementary Figure 22a,b,e,f** for DRG neurons.

	Nodose ganglion	DRG
Capsaicin-responding cells;		
WT	48.5% (81/167)	41.3% (102/247)
Trpa1 KO	45.5% (102/224)	39.1% (61/156)
Hyperoxia-responding cells;		
WT	28.6% (8/28)	40.0% (32/80)
Trpa1 KO	4.84% (3/62)	12.1% (4/33)
Hyperoxia- and capsaicin-responding cells;		
WT	25.0% (7/28)	25.0% (20/80)
Trpa1 KO	0.02% (1/62)	0.03% (1/33)
Hypoxia-responding cells;		
WT	12.2% (17/139)	21.6% (36/167)
Trpa1 KO	3.09% (5/162)	7.31% (9/123)
Hypoxia- and capsaicin-responding cells;		
WT	12.2% (17/139)	10.8% (18/167)
Trpa1 KO	0.00% (0/162)	0.81% (1/123)

Supplementary Table 3. Primer sequences used for overlap extension PCR in producing mutants.

Genes	Mutants	Mutation primer sequences (5'→ 3')	External primer sequences (5' → 3')	Restriction sites used for cloning into TRPA1-pCIneo, PHD1-pCIneo, PHD2-pCIneo or PHD3-pCIneo
TRPA1	C3S	for: CTTCCACCATGAAGAGCAGCCTGAGGAAG rev: CATCTTCCTCAGGCTGCTCTTCATGGTG	for: CTGCAGTGACTCTCTTAAGGTAGCCTTG rev: CTGTCTACATGCATAATGTAGAGGAGTACAC	*Xho*I / *Nhe*I
	C59S	for: GAAATTAAAAACAAGTGACGATATGGAC rev: GTCCATATCGTCACTTGTTTTTAATTTC		
	C104S	for: GGAAATACCCCTCTGCATAGTGCTGTAG rev: CTACAGCACTATGCAGAGGGGTATTTCC		
	C173S	for: GATCATTGCGAGCACCACAAATAATAG rev: TATTTGTGGTGCTCGCAATGATCACAG		
	C192S	for: GGAGCTAAGCCAAGTAAATCAAATAAATG rev: CATTTATTTGATTTACTTGGCTTAGCTCC		
	C199S	for: GGAAGTTTCCCTATTCACCAAGCTGC rev: GCAGCTTGGTGAATAGGGAAACTTCC		
	C213S	for: GGTTCCAAAGAAAGCATGGAAATAATAC rev: GTATTATTTCCATGCTTTCTTTGGAACC		
	C258S	for: GATCAAAATGAGCCTGGACAATGGTG rev: GTGCACCATTGTCCAGGCTCATTTTG		
	C273S	for: GAAGGGAAGGAGCACAGCCATTCATTTTG rev: AATGAATGGCTGTGCTCCTTCCCTTCTC		
	C308S	for: CAACCGATGGAAGTCATGAGACCATGC rev: GCATGGTCTCATGACTTCCATCGGTTG		
TRPA1	C462S	for: GTATCAATACCAGTCAGAGGCTCCTACAAG rev: CTTGTAGGAGCCTCTGACTGGTATTGATACG	for: ACCGATGGATGTCATGAGACCATGCTTC rev: GCAATGTCGCCAACTGCCAAACCAATAAG	*Apa*I / *Bam*HI
	C608S	for: GATGGGATGAAAGTCTTAAGATTTTCAGTC rev: GACTGAAAATCTTAAGACTTTCATCCCATC		
	C633S	for: CTCCCTGAAAGCATGAAGGTACTTTTAG rev: GTACCTTCATGCTTTCAGGGAGGTATTC		
	C651S	for: GACAAGTCCAGCCGAGACTATTATATC rev: GATATAATAGTCTCGGCTGGACTTGTCTTC		
	C703S	for: CTGTGAGTAAAGAATATTTACTCATGAAATGG rev: CCATTTCATGAGTAAATATTCTTTACTCACAG		
	C727S	for: GATGAATTTAGGATCTTACAGTCTTGGTCTC rev: AAGACTGTAAGATCCTAAATTCATCATATGAG		
	C773S	for: CCACGAATTCATATCTAATAAAAACTAGTATG rev: CATACTAGTTTTTATTAGATATGAATTCGTGG		
	C786S	for: GTATATTTGGGTATAGCAAAGAAGCGGG rev: CCCGCTTCTTTGCTATACCCAAATATAC		
	C834S	for: GTGGCAAAGTGGAGCAATTGCTGTTTAC rev: GTAAACAGCAATTGCTCCACTTTGCCAC		
	C856S	for: CAAAGATTTGAAAATAGTGGAATTTTTATTG rev: ATTCCACTATTTTCAAATCTTTGAAGATAC		
TRPA1	C1021S	for: CCATATATTCAGTTTTTTATTTTGCACTGG rev: CCAGTGCAAAATAAAAAACTGAATATATGG	for: CTCAGCTTTTACATCCTCCTGAATTTAC rev: CCTTATCGGATTTTACCACATTTGTAGAG	*Bam*HI / *Xma*I
	C1025S	for: CTGTTTTTTATTTAGCACTGGGGAAATAAG rev: CTTATTTCCCCAGTGCTAAATAAAAAACAG		
	C1085S	for: GATGATGATAGCCATAGTTCTTTTCAAGAC rev: GTCTTGAAAAGAACTATGGCTATCATCATC		
PHD1	H357A	for: GAACCCCGCCGAGGTGAAGCCAGCCTATGC rev: GCATAGGCTGGCTTCACCTCGGCGGGGTTC	for: CACGAATTCTCCACCATGGACAGCCCGTGCCAGCC rev: CACGTCGACCTAGGTGGGCGTAGGCGGCTGTG	*Eco*RI / *Sal*I
PHD2	H374A	for: TCGCAACCCTGCTGAAGTACAACCA rev: TGGTTGTACTTCAGCAGGGTTGCGA	for: CACGAATTCTCCACCATGGCCAATGACAGCGGCG rev: CACGTCGACCTAGAAGACGTCTTTACCGAC	*Eco*RI / *Sal*I
PHD3	H196A	for: CGTAGGAACCCAGCCGAAGTGCAG rev: CTGCACTTCGGCTGGGTTCCTACG	for: CACGAATTCTCCACCATGCCCCTGGGACACATCAT rev: CACGTCGACTCAGTCTTCAGTGAGGGCAG	*Eco*RI / *Sal*I
TRPA1	P394A	for: TGCGAGCTGAATTTATGCAGATGCAACA rev: TGTTGCATCTGCATAAATTCAGCTCGCA	for: ACTCACTATAGGCTAGCCTCGAGAATTCGGG rev: CTTGTAGGAGCCTCTGACAGGTATTGATACG	*Xho*I / *Apa*I

for: forward primer rev: reverse primer

Supplementary Table 4. Primer sequences used in RT-PCR experiments.

Species	Genes	Primer sequences (5' → 3')
Mouse	PHD1	for: ACCGCGCAGCATTCGTG rev: GGGGCTGGCCATTAGGTAGGTGTA
Mouse	PHD2	for: GCGGGAAGCTGGGCAACTAC rev: TCAACCCTCACACCTTTCTCACC
Mouse	PHD3	for: CTGCGTGCTGGAGCGAGTCAA rev: TCATGTGGATTCCTGCGGTCTG
Mouse	β-actin	for: GATGACGATATCGCTGCGCTG rev: GTACGACCAGAGGCATACAGG
Human	PHD1	for: GGCGATCCCGCCGCGC rev: CCTGGGTAACACGCCACC
Human	PHD2	for: GCACGACACCGGGAAGTT rev: CCAGCTTCCCGTTACAGT
Human	PHD3	for: GGCCATCAGCTTCCTCCTG rev: GGTGATGCAGCGACCATCA
Human	β-actin	for: CATCCGCAAAGACCTGTACGCCAACAC rev: CTCGTCATACTCCTGCTTGCTGATCCAC

for: forward primer rev: reverse primer

Supplementary References

1. Yoshida, T. *et al.* Nitric oxide activates TRP channels by cysteine S-nitrosylation. *Nat. Chem. Biol.* **2,** 596–607 (2006).
2. Jobling, S.A. & Gehrke, L. Enhanced translation of chimaeric messenger RNAs containing a plant viral untranslated leader sequence. *Nature* **325,** 622–625 (1987).
3. Kozak, M. Point mutations define a sequence flanking the AUG initiator codon that modulates translation by eukaryotic ribosomes. *Cell* **44,** 283–292 (1986).
4. Ho, S.N., Hunt, H.D., Horton, R.M., Pullen, J.K. & Pease, L.R. Site-directed mutagenesis by overlap extension using the polymerase chain reaction. *Gene* **77,** 51–59 (1989).
5. Takahashi, N. *et al.* Molecular characterization of TRPA1 channel activation by cysteine-reactive inflammatory mediators. *Channels (Austin)* **2,** 287–298 (2008).
6. Metzen, E., Zhou, J., Jelkmann, W., Fandrey, J. & Brüne, B. Nitric oxide impairs normoxic degradation of HIF-1α by inhibition of prolyl hydroxylases. *Mol. Biol. Cell* **14,** 3470–3481 (2003).
7. Klein, A., Flügel, D. & Kietzmann, T. Transcriptional regulation of serine/threonine kinase-15 (STK15) expression by hypoxia and HIF-1. *Mol. Biol. Cell* **19,** 3667–3675 (2008).
8. Lee, S. *et al.* Neuronal apoptosis linked to EglN3 prolyl hydroxylase and familial pheochromocytoma genes: developmental culling and cancer. *Cancer Cell* **8,** 155–167 (2005).
9. Monet, M. *et al.* Lysophospholipids stimulate prostate cancer cell migration via TRPV2 channel activation. *Biochim. Biophys. Acta* **1793,** 528–539 (2009).
10. Hu, H., Grandl, J., Bandell, M., Petrus, M. & Patapoutian, A. Two amino acid

residues determine 2-APB sensitivity of the ion channels TRPV3 and TRPV4. *Proc. Natl. Acad. Sci. USA* **106,** 1626–1631 (2009).

11. Hara, Y. *et al.* LTRPC2 Ca^{2+}-permeable channel activated by changes in redox status confers susceptibility to cell death. *Mol. Cell* **9,** 163–173 (2002).
12. Kiyonaka, S. *et al.* Selective and direct inhibition of TRPC3 channels underlies biological activities of a pyrazole compound. *Proc. Natl. Acad. Sci. USA* **106,** 5400–5405 (2009).
13. Okada, T. *et al.* Molecular cloning and functional characterization of a novel receptor-activated TRP Ca^{2+} channel from mouse brain. *J. Biol. Chem.* **273,** 10279–10287 (1998).
14. Numata, T., Shimizu, T. & Okada, Y. Direct mechano-stress sensitivity of TRPM7. *Cell Physiol. BioChem.* **19,** 1–8 (2007).
15. Petrus, M. *et al.* A role of TRPA1 in mechanical hyperalgesia is revealed by pharmacological inhibition. *Mol. Pain* **3,** 40 (2007).
16. Shi, M. & Liu, Y.H. Traditional Morita–Baylis–Hillman reaction of aldehydes with methyl vinyl ketone co-catalyzed by triphenylphosphine and nitrophenol. *Org. Biomol. Chem.* **4,** 1468–1470 (2006).
17. Yi, H.W., Park, H.W., Song, Y.S. & Lee, K.J. Reaction of the Morita–Baylis–Hillman acetates of 2-azidobenzaldehydes with triethyl phosphite: synthesis of 1-diethylphosphono-1,2-dihydroquinolines and 3-acetoxymethylquinolines. *Synthesis* 1953–1960 (2006).
18. Pachamuthu, K. & Vankar, Y.D. Palladium catalysed regio and stereoselective reduction of Baylis-Hillman coupling products derived allylic acetates. *Tetrahedron Lett.* **39,** 5439–5442 (1998).

19. Okada, T. *et al.* Molecular and functional characterization of a novel mouse transient receptor potential protein homologue TRP7. Ca^{2+}-permeable cation channel that is constitutively activated and enhanced by stimulation of G protein-coupled receptor. *J. Biol. Chem.* **274,** 27359–27370 (1999).
20. Cockman, M.E., Webb, J.D., Kramer, H.B., Kessler, B.M. & Ratcliffe, P.J. Proteomics-based identification of novel factor inhibiting hypoxia-inducible factor (FIH) substrates indicates widespread asparaginyl hydroxylation of ankyrin repeat domain-containing proteins. *Mol. Cell Proteomics* **8,** 535–546 (2008).
21. Kwan, K.Y. *et al.* TRPA1 contributes to cold, mechanical, and chemical nociception but is not essential for hair-cell transduction. *Neuron* **50,** 277–289 (2006).
22. Aragonés, J. *et al.* Deficiency or inhibition of oxygen sensor Phd1 induces hypoxia tolerance by reprogramming basal metabolism. *Nat. Genet*. **40,** 170–180 (2008).
23. Bishop, T. *et al.* Abnormal sympathoadrenal development and systemic hypotension in PHD3-/- mice. *Mol. Cell Biol.* **28,** 3386–3400 (2008).
24. Nagatomo, K. & Kubo, Y. Caffeine activates mouse TRPA1 channels but suppresses human TRPA1 channels. *Proc. Natl. Acad. Sci. USA* **105,** 17373–17378 (2008).
25. Harlow, E. & Lane, D. *Using antibodies: a laboratory manual.* (Cold Spring Harbor Laboratory Press, New York, 1999).